

---

---

**REPORT No. 255**

---

**PRESSURE DISTRIBUTION OVER AIRFOILS AT  
HIGH SPEEDS**

**By L. J. BRIGGS and H. L. DRYDEN.**  
Bureau of Standards



# REPORT No. 255

## PRESSURE DISTRIBUTION OVER AIRFOILS AT HIGH SPEEDS

By L. J. BRIGGS and H. L. DRYDEN

### SUMMARY

This report deals with the pressure distribution over airfoils at high speeds, and describes an extension of an investigation of the aerodynamic characteristics of certain airfoils which was presented in N. A. C. A. Technical Report No. 207 (Reference 1). The work was carried out at the request and with the financial assistance of the National Advisory Committee for Aeronautics. A large compressor plant at Edgewood Arsenal was made available for the experiments through the courtesy of the Chemical Warfare Service.

The results presented in Report No. 207 have been confirmed and extended to higher speeds through a more extensive and systematic series of tests. Observations were also made of the air flow near the surface of the airfoils, and the large changes in lift coefficients were shown to be associated with a sudden breaking away of the flow from the upper surface.

The tests were made on models of 1-inch chord and comparison with the earlier measurements on models of 3-inch chord shows that the sudden change in the lift coefficient is due to compressibility and not to a change in the Reynolds Number. The Reynolds Number still has a large effect, however, on the drag coefficient.

The pressure distribution observations furnish the propeller designer with data on the load distribution at high speeds, and also give a better picture of the air-flow changes.

### INTRODUCTION

In Technical Report 207 of the National Advisory Committee for Aeronautics an account is given of the results of some measurements by G. F. Hull and the authors of the lift, drag, and center of pressure of six airfoils at speeds ranging from 550 to 1,000 feet per second. The airfoils were of the type used by the Army Air Service in the design of wooden propellers, and the experiments showed that their aerodynamic characteristics at the speeds actually encountered in propeller blades were quite different from those at ordinary wind tunnel speeds.

The present report describes an extension of the investigation to the measurement of the distribution of pressure over the same six airfoil sections at high speeds. The object of this additional work was twofold; first, to furnish the designer with data on the load distribution at high speeds, and second, to throw some light on the changes in air flow, so that a better understanding might be gained of the effect of high speeds on the type of air flow.

The work described in Report No. 207 was carried out in an air stream 12 inches in diameter at the Lynn plant of the General Electric Co., on airfoils of 3-inch chord. It was not possible to continue the work at Lynn, because no compressor was available. Furthermore, the operating conditions at Lynn were such that it was difficult to obtain a series of observations at the same wind speed without a large expenditure of time. It was decided therefore to carry on the work at the compressor plant at Edgewood Arsenal in an air stream 2 inches in diameter and on models of 1-inch chord, the plant being made available through the courtesy of the Chemical Warfare Service. Although this change in the size of the model and the air stream had the disadvantage of changing the experimental conditions so that the results were not exactly comparable, the modification of the program has amply justified itself by the marked improvement in operating conditions and it has, in addition, given new information as to the relative importance of the viscosity and compressibility effects.

## APPARATUS

*Air stream.*—The air stream was furnished by the 155-millimeter compressor plant at Edgewood Arsenal. This plant, which was used during the war in connection with the refrigeration of mustard gas during the process of filling gas shells, consists of four electrically-driven double-acting reciprocating compressors capable of delivering jointly about 1,800 cubic feet of free air per minute at any pressure up to 125 pounds per square inch. In the present work they were used to maintain an air stream at a speed up to 1,250 feet per second through a 2-inch orifice. The air after leaving the compressors was water-cooled and then passed through a 4-inch line in which a tank was included to damp out the pulses produced by the reciprocating motion of the compressors. About 200 feet along the line from the compressors the air passed into a vertical pipe 8 inches in diameter, with an orifice mounted at its upper end for forming the high-speed air jet. The air speeds at which observations were taken were 0.5, 0.65, 0.8, 0.95, and 1.08 times the speed of sound at the temperature of the jet, corresponding to 563, 732, 902, 1,071, and 1,218 feet per second at 20° C. The pressure and therefore the jet speed was maintained constant by a manually operated blow-off valve placed in a line connected to the ballast tank mentioned above. The values of the air speed were computed from the pressure observed on a manometer connected to a small hole in the 8-inch pipe about 2 feet ahead of the orifice mouth, the method of computation being described in the section on reduction of observations.

*Orifices.*—Two orifices were used. For speeds below the speed of sound a 2-inch cylindrical orifice, 1.05 inches in length, was found to give satisfactory flow conditions. For the highest speed of 1.08 times the speed of sound it was necessary to use a slightly expanding orifice to avoid large fluctuations in pressure in the stream. This orifice had a throat diameter of 1.9 inches, a length of 0.55 inches, and a taper of about 1 in 21. In each case a rounded approach was used, the section being changed from the full 8-inch diameter of the pipe to the throat diameter in a length of about  $4\frac{3}{4}$  inches.

*Airfoils.*—The airfoil sections were the same as those described in detail in Technical Report No. 207 of the National Advisory Committee for Aeronautics but were of 1-inch chord. (Cf. figs. 4–9.) The maximum thickness was 0.10, 0.12, 0.14, 0.16, 0.18, and 0.20 inch, respectively, for the six airfoils. Because of the small thickness it was not practicable to have enough stations on one airfoil to determine the pressure distribution satisfactorily, for the forces involved were rather large and the insertion of connecting tubes necessitated the removal of a comparatively large amount of metal. For this reason seven models were required for each of the six sections. They were made by Mr. W. H. Nichols, of Waltham, Mass., and were of brass, to facilitate the necessary machining operations.

Thirteen stations were chosen as a minimum number satisfactory for determining the pressure distribution curves. Seven stations were placed on the upper surface and six on the lower, spaced close together near the leading edge where large pressure changes were to be anticipated. The locations of the stations with regard to the airfoil section are shown in Table I which gives the distance of each station from the nose, measured parallel to the chord and expressed as a fraction of the chord. The ordinates at these points are given for airfoil No. 1 of 0.10 camber ratio, and the values for the other airfoils are proportional to the camber ratio. The lower surfaces of all the airfoils were plane.

TABLE I  
UPPER SURFACE

Station	Distance from nose	Ordinate for airfoil 1
1.....	0.025	0.041
2.....	0.050	0.059
3.....	0.100	0.079
4.....	0.200	0.095
5.....	0.400	0.097
6.....	0.600	0.087
7.....	0.850	0.045

LOWER SURFACE

8.....	0.050	0.000
9.....	0.100	0.000
10.....	0.200	0.000
11.....	0.400	0.000
12.....	0.600	0.000
13.....	0.850	0.000

Two stations were located on each of six models of each airfoil section, while one model carried only one station. The holes (about 0.025 inch in diameter) were offset one-eighth inch from the center of the airfoil, one toward either end, and connection was made through small tubing set into a groove milled in the opposite surface of the airfoil to short tubes of larger diameter soldered to the ends of the airfoil. After the tubing had been placed, the groove was filled with solder and carefully smoothed over. Figure 1 shows a number of the models with end connections.

*Airfoil mounting.*—A flange on the vertical 8-inch pipe carried two vertical rods, which served as supports. (See fig. 3.) The mounting for the airfoils is shown in Figure 2. The semicircular bracket B, forming the main part of the mounting, could be rotated at O about one of the vertical rods, so that the airfoil could be swung into the stream or taken out at will. The bracket carried two hollow members M rotating in plain bearings about a common horizontal axis and shaped so that the airfoil A could be clamped firmly to them at each end. The rotating members carried pointers P traveling over angular scales fastened to the bracket. A



FIG. 1.—Two groups of airfoils used in the tests. The holes for measuring the pressure may be seen on airfoil 2-5, 2-4

tangent screw S provided a close adjustment, and quick acting clamps C held the airfoil in position at any angle to the air stream. Rubber tubing connections to a manometer were brought in through the hollow rotating members to the short metal tubes on the ends of the airfoil.

*Manometers.*—The static pressure in the 8-inch pipe was measured by means of a dead-weight piston gauge or by a mercury U-tube gauge. The two instruments were connected in parallel, so that either could be used or the two compared at any time. The U-tube gauge proved better for low pressures and speeds, while the dead-weight gauge was satisfactory at the two higher speeds.

The pressure at the station on the airfoil was read on a mercury U-tube gauge of special design. The instrument was provided with markers designed to avoid parallax and so arranged that the markers could be set quickly and the actual scale readings taken subsequently while a new pressure was building up. The U-tube was also equipped at the bend with a valve which could be used to hold the mercury in position while adjustments were being made on the airfoil. The valve could also be used to damp out fluctuations by partially closing it, but this was found necessary in only a few instances.

Both pressures were measured with reference to the actual barometric pressure since static tube measurements showed that the static pressure of the stream was equal to the barometric pressure, within the experimental error. The barometric pressure was measured by a standard mercurial barometer.

Thermometers were provided to measure the air temperature in the pipe and the air temperature near the manometers and barometer.

A general view of the set-up is shown in Figure 3.

#### GENERAL PROCEDURE

The measurements were carried out in the following order. A model was clamped in the support and set at an angle of zero degrees to the wind stream. One station was connected to the mercury U-tube, and the connection to the other station closed. The airfoil was then swung into the air stream and the manometer allowed to come to a steady state. The valve on the manometer was then closed and the observer at the manometer adjusted the markers while the observer at the airfoil turned the airfoil to a new angle. After the markers were set, the first observer opened the manometer valve and read the position of the markers and recorded them while equilibrium in the new condition was being established. Measurements were made for this one station at the lowest speed at 4° intervals from -20° to +24°. The second station was then connected and the first closed off and measurements made over the same range of angles. The airfoil was then removed and a replica with two other stations carried through the same range, this process being continued until all 13 stations on one section had been covered at one speed, a total of 156 observations.

The remaining five sections were tested at the same speed, making 936 observations, and then the whole series was repeated for each of the remaining four speeds, giving 4,680 observations in all. Where necessary, additional observations were interpolated.

An assistant kept the pressure in the 8-inch pipe constant by hand regulation of the blow-off valve and thus, as will be shown later, kept the value of the ratio of the air speed to the speed of sound constant at the desired value.

#### REDUCTION OF OBSERVATIONS

*Notation.*—

$p$  = absolute pressure at a station on the airfoil.

$p_1$  = absolute static pressure inside pipe (velocity pressure negligible).

$p_o$  = absolute static pressure in jet (equal to barometric pressure).

$p_1 - p_o$  = impact pressure.

$V$  = the speed of air in jet.

$c$  = speed of sound at temperature of jet.

$\rho$  = density of air in jet.

$\mu$  = viscosity of air in jet.

$q = \frac{1}{2} \rho V^2$  = velocity pressure.

$l$  = linear dimension determining the scale (chord of airfoil).

$J$  = mechanical equivalent of heat.

$C_p$  = specific heat of air at constant pressure.

$k$  = ratio of specific heats.

$T_1$  = absolute temperature in pipe before expansion.

$T_o$  = absolute temperature in jet after expansion.

*Pressure on airfoils.*—The results of the pressure measurements are expressed in terms of the nondimensional or absolute coefficients of the type described in Report 207 of the National Advisory Committee for Aeronautics. The principle of dimensional homogeneity indicates that the pressure difference  $p - p_o$  is equal to the velocity pressure,  $q = \frac{1}{2} \rho V^2$ , times a function of the Reynolds Number  $Vl\rho/\mu$  and the compressibility variable  $V/c$ . In other words

$$\frac{p - p_o}{\frac{1}{2} \rho V^2} = \frac{p - p_o}{q} = f\left(\frac{Vl}{\mu}, \frac{V}{c}\right)$$

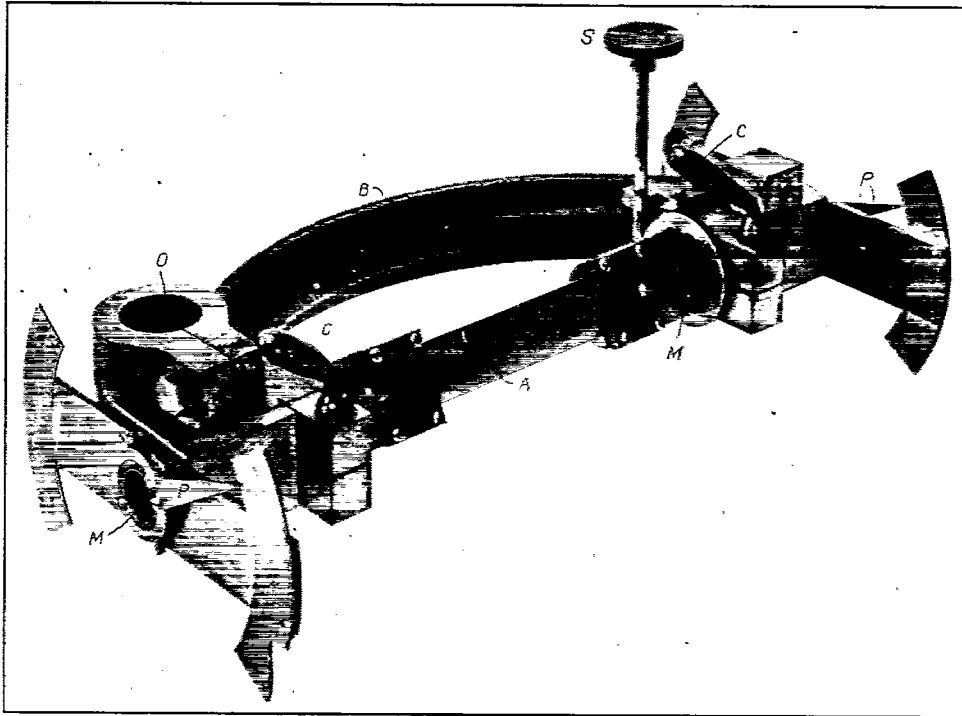


FIG. 2.—The apparatus for holding the airfoil

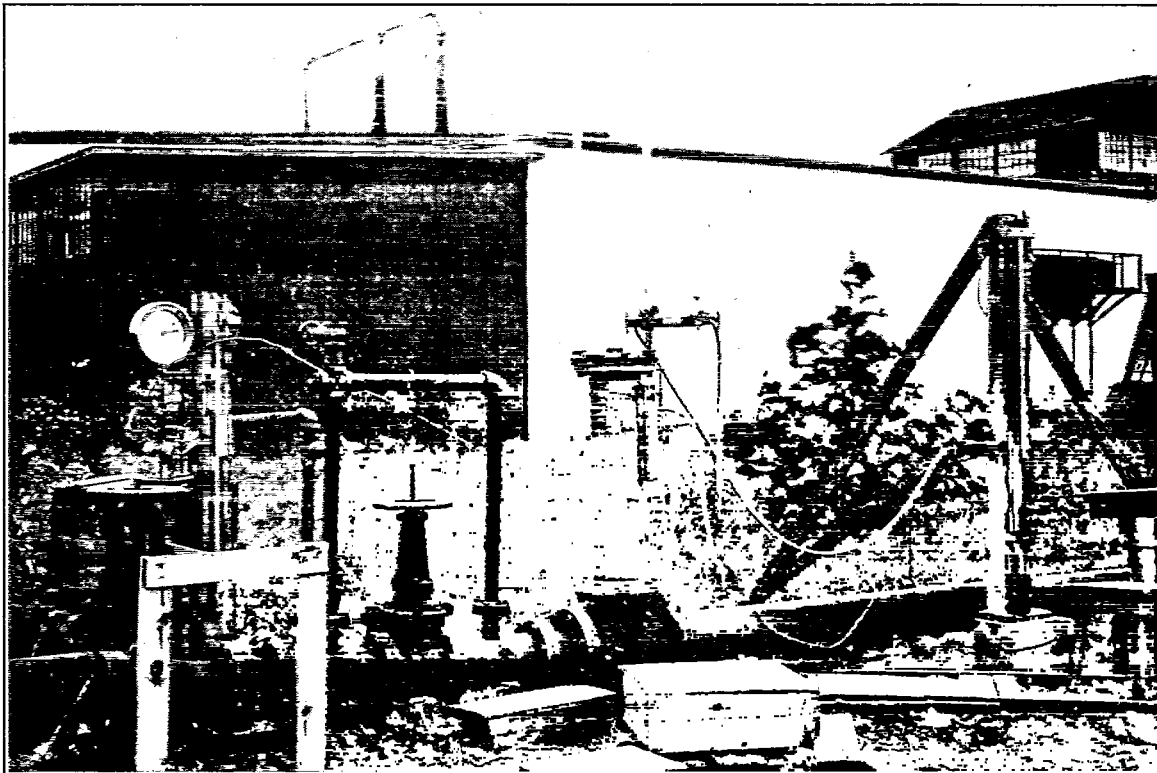


FIG. 3.—General view of apparatus. Gauges for speed measurement and control valves at the left, airfoil mounting in the center, gauge for pressure distribution at the right

As will be shown in the next paragraph  $q$  is equal to the measured pressure in the 8-inch pipe times a factor which depends only on the speed ratio,  $\frac{V}{a}$ . Both  $p$  and the pipe pressure are measured on mercury manometers at nearly the same temperature for the three low speeds so that the ratio may be taken directly without further reduction. For the two high speeds the reading of the dead-weight gauge is first reduced to cm. of Hg. Values of  $\frac{p-p_o}{q}$  are then obtained by multiplying by the appropriate factor of Table II.

*Speed ratio.*—The speed ratio is computed from the pressure of the air in the pipe before expansion on the assumption that the expansion through the orifice is isentropic, that air is an ideal gas, and that the pressure in the jet just outside the orifice is equal to the barometric pressure. The first assumption is substantiated by the experimental fact that for speeds below the speed of sound an impact tube in the jet gives a pressure which balances the pressure on an impact tube in the pipe within very close limits. Hence there is no appreciable dissipation of energy by resistance or heat conduction, during the expansion through the nozzle and the recompression ahead of the impact tube in the jet. The third assumption is substantiated by static tube measurements in the jet.

The formula for the speed computed on these assumptions is

$$V^2 = 2JC_p T_i \left\{ 1 - \left( \frac{p_o}{p_i} \right)^{\frac{k-1}{k}} \right\} = 2JC_p (T_i - T_o) \quad (1)$$

Now the velocity of sound  $c$  is proportional to the square root of the absolute temperature; hence if  $c_o$  is the value under standard conditions, as for example at 0° C,

$$c = c_o \sqrt{\frac{T_o}{273}}$$

Since

$$T_o = T_i \left( \frac{p_o}{p_i} \right)^{\frac{k-1}{k}}$$

$$c^2 = \frac{c_o^2 T_i}{273} \left( \frac{p_o}{p_i} \right)^{\frac{k-1}{k}}$$

Dividing equation (1) by  $c^2$

$$\frac{V^2}{c^2} = \frac{546JC_p}{c_o^2} \left\{ \left( \frac{p_i}{p_o} \right)^{\frac{k-1}{k}} - 1 \right\} \quad (2)$$

$V/c$  therefore depends only on the absolute pressure ratio and not on the temperature  $T_i$ .

The values of  $p_i - p_o$  corresponding to a definite value of  $V/c$  vary slowly with changes in the barometric pressure,  $p_o$ , but it was found quite feasible to make allowance for this variation and carry out all measurements at the same value of  $V/c$ . The effect of change of the density of mercury with temperature was well within the general precision of the work.

Attention has been called to the fact that the velocity pressure  $\frac{1}{2}\rho V^2$  may be readily computed from the observed pressure,  $p_i - p_o$ . In fact

$$\rho = \frac{p_o}{T_o} \frac{288 \times 0.0012255}{1\ 013\ 300}$$

where  $\rho$  is the density in gm/cm<sup>3</sup>,  $p_o$  the barometric pressure in dynes/cm<sup>2</sup> and  $T_o$  the absolute temperature in °C. Hence

$$\frac{1}{2}\rho V^2 = \frac{288 \times 0.0012255}{1\ 013\ 300} JC_p p_o \left\{ \left( \frac{p_i}{p_o} \right)^{\frac{k-1}{k}} - 1 \right\}$$

Substituting for the quantity in the brackets its equivalent from equation (2)

$$\frac{1}{2} \rho V^2 = 3.5088 p_o (0.19991 V^2/c^2)$$

Therefore

$$\frac{p_i - p_o}{\frac{1}{2} \rho V^2} = \frac{\frac{p_i}{p_o} - 1}{3.5088 \times 0.19991 \frac{V^2}{c^2}} = \frac{\left(1 + 0.19991 \frac{V^2}{c^2}\right)^{7/2} - 1}{3.5088 \times 0.19991 \frac{V^2}{c^2}} \quad (3)$$

a result dependent only on  $V/c$ . Values for the speeds used are given in Table II and by their aid the results given in the paper for  $\frac{p - p_o}{\frac{1}{2} \rho V^2}$  can be recomputed to give ratios to impact pressure  $p_i - p_o$  if desired.

TABLE II

$\frac{V}{c}$	$\frac{p_i - p_o}{\frac{1}{2} \rho V^2}$
0.50	1.061
0.65	1.107
0.80	1.170
0.95	1.244
1.08	1.325

The tables in the appendix to this report and the curves of Figures 4 to 9 give the values of  $\frac{p - p_o}{\frac{1}{2} \rho V^2}$  for the 13 stations on each of the six airfoil sections at the five values of  $\frac{V}{c}$ .

#### INTEGRATION OF PRESSURES

For comparison with the earlier results it is necessary to compute values of the total forces and moments, i. e., the lift coefficients, drag coefficients, and center of pressure coefficients as defined in Report 207.<sup>1</sup>

It is inconvenient to determine the lift and drag coefficients directly and therefore the normal force and tangential force coefficients,  $C_N$  and  $C_T$  are first computed, the normal force being defined as the force normal to the chord of the airfoil (whereas the lift is normal to the wind direction) and the tangential force as the force parallel to the chord (whereas the drag is parallel to the wind direction). The lift and drag coefficients,  $C_L$  and  $C_D$ , follow immediately from the relations

$$\begin{aligned} C_L &= C_N \cos \alpha - C_T \sin \alpha \\ C_D &= C_N \sin \alpha + C_T \cos \alpha \end{aligned}$$

where  $\alpha$  is the angle of attack.

Forces computed from the observed pressures can not take account of the effects of skin friction, since only the pressure normal to the surface is measured by the method described. It is to be expected, therefore, that the forces computed from the pressures will differ somewhat from the directly measured forces, especially in the case of the drag component.

The method of determining the normal and tangential force coefficients from the pressures normal to the surface reduces to the determination of the area of two curves, one in which the observed pressures are plotted as ordinates and distances of the station parallel to the chord

$$\begin{aligned} C_L &= \frac{\text{Lift}}{\frac{1}{2} \rho V^2 \text{ Area}} \\ C_D &= \frac{\text{Drag}}{\frac{1}{2} \rho V^2 \text{ Area}} \end{aligned}$$

<sup>1</sup> Center of pressure coefficient = distance center of pressure to leading edge measured parallel to chord divided by chord length.  
Moment coefficient =  $(C_L \cos \alpha + C_D \sin \alpha)$  times center of pressure coefficient  
 $\alpha$  = angle of attack.

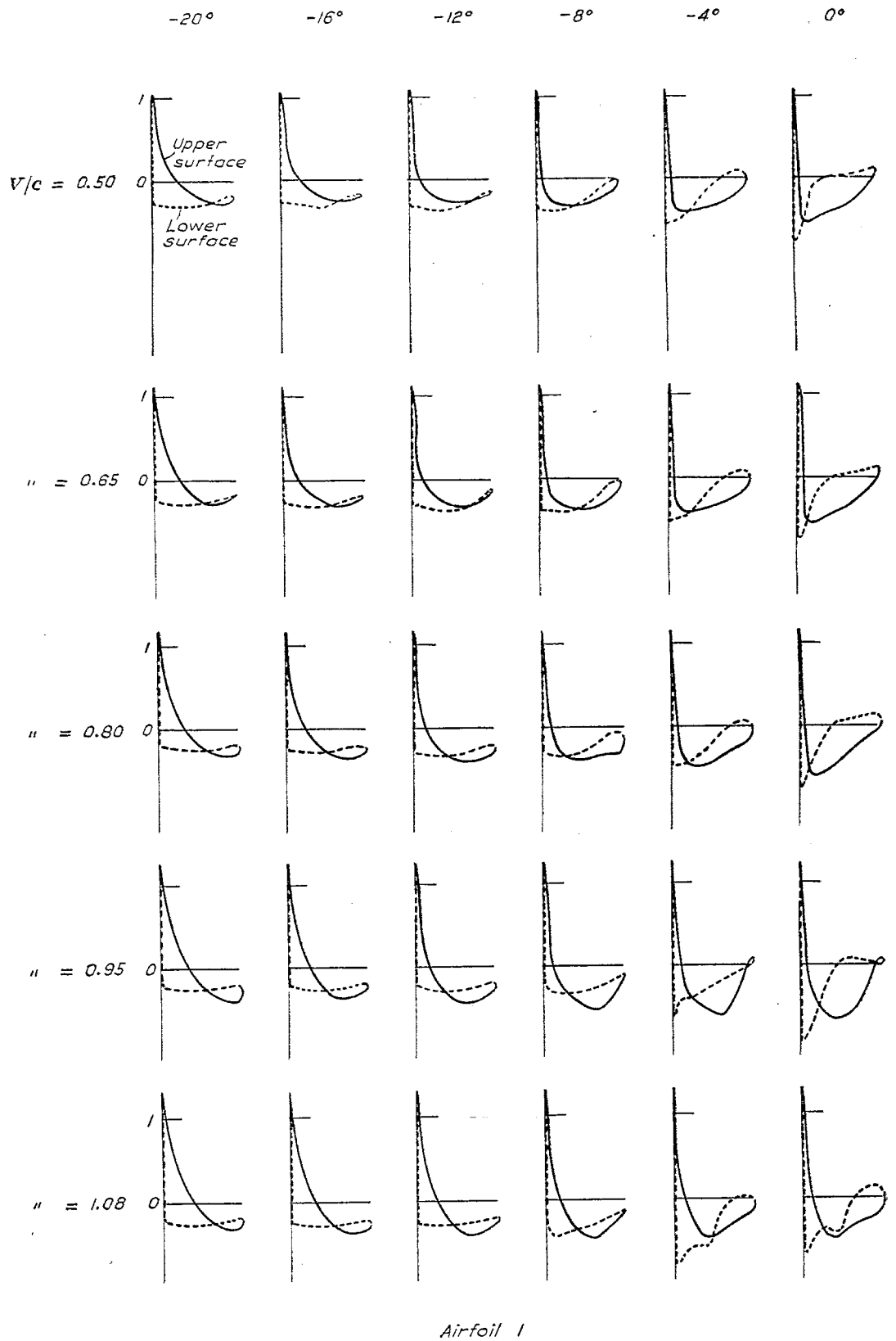
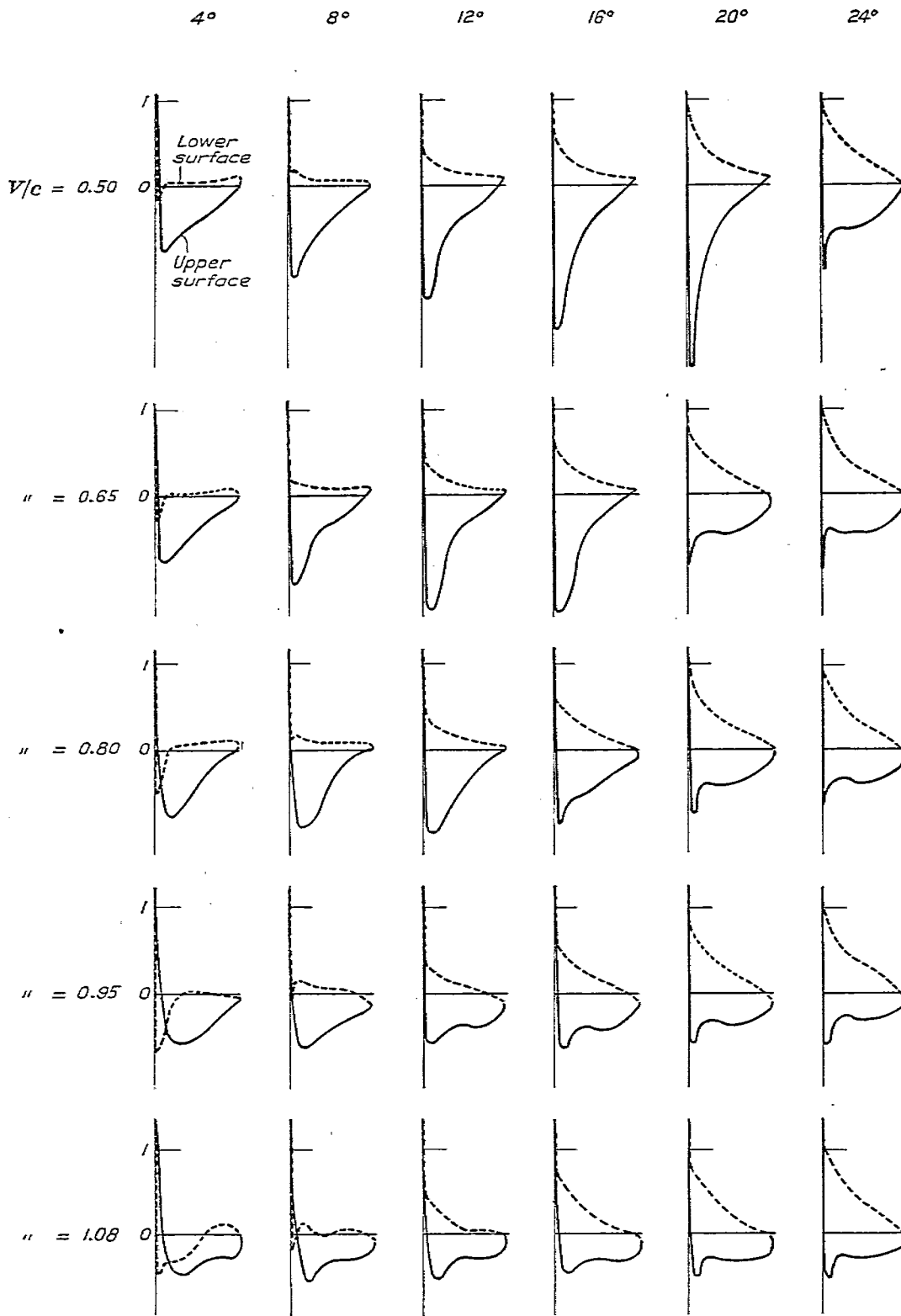


FIG. 4.—Distribution of pressure over airfoil 1 at various speeds and angles. Abscissae are distances from the nose measured along the chord. Ordinates are values of  $\frac{p-p_0}{\frac{1}{2}\rho V^2}$



Airfoil 1

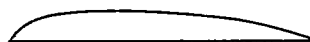


Fig. 4.—Continued

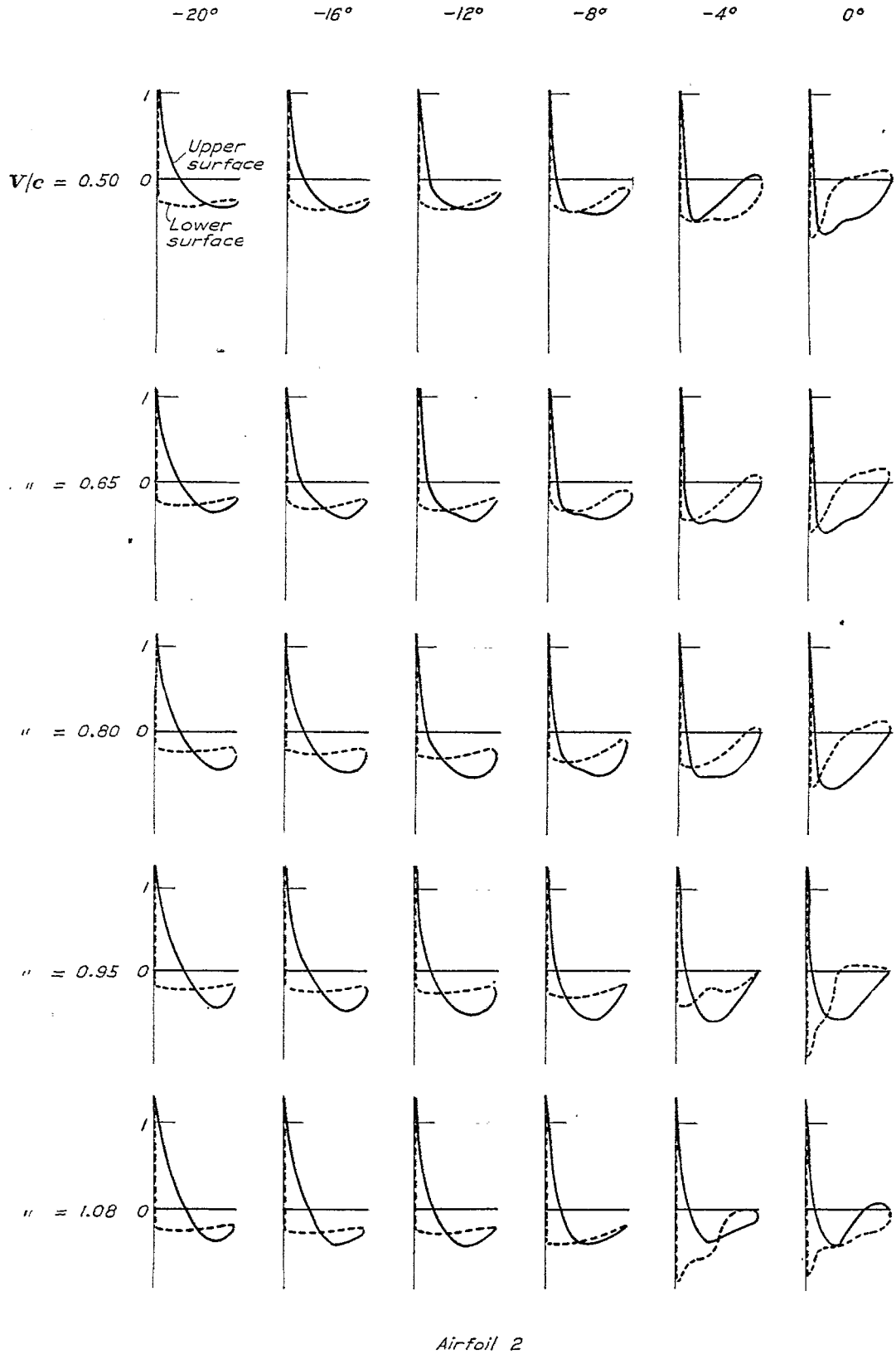
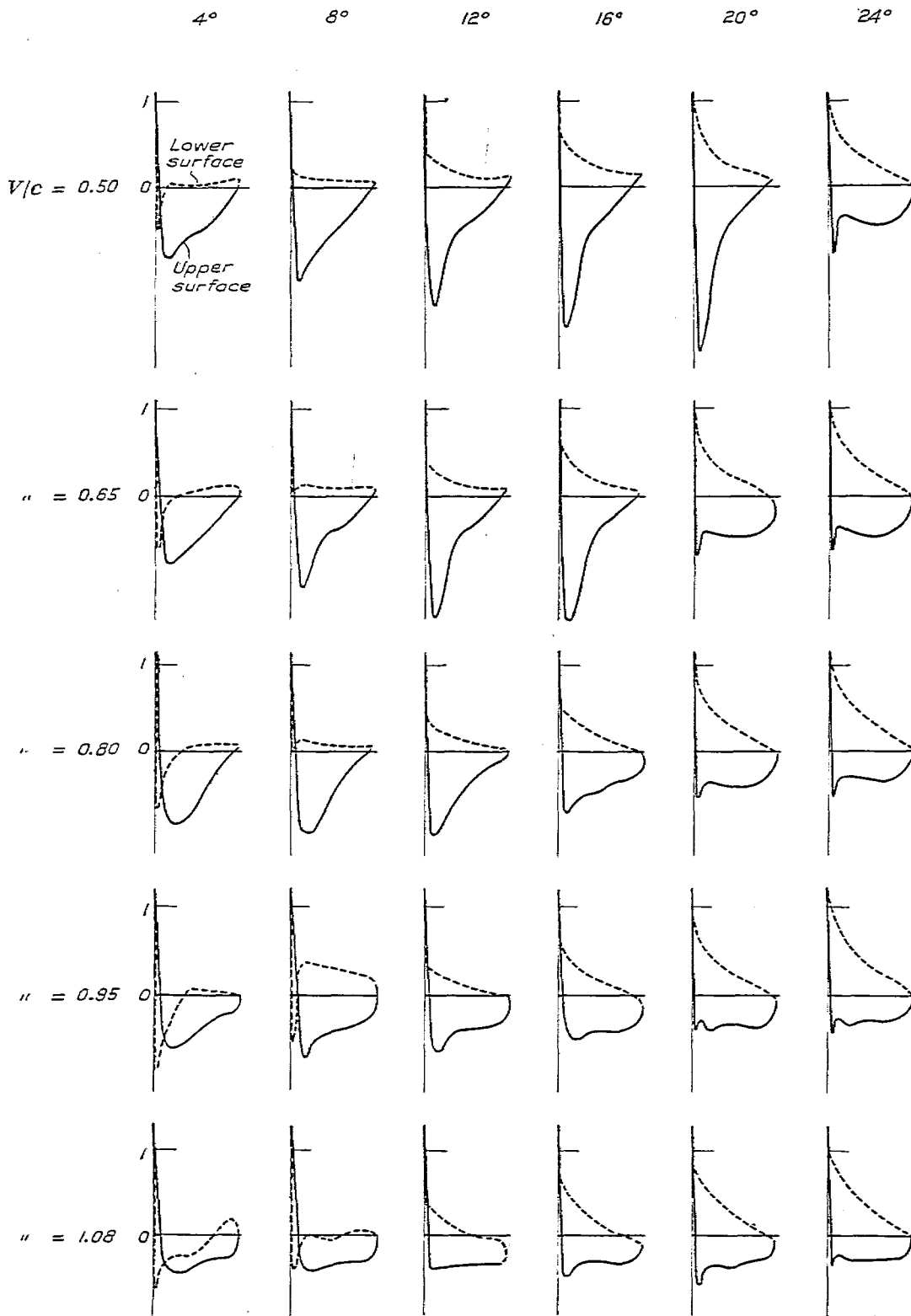


Fig. 5.—Distribution of pressure over airfoil 2 at various speeds and angles. Abscissae are distances from the nose measured along the chord. Ordinates are values of  $\frac{p-p_0}{\frac{1}{2}\rho V^2}$



Airfoil 2

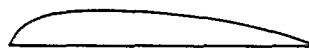
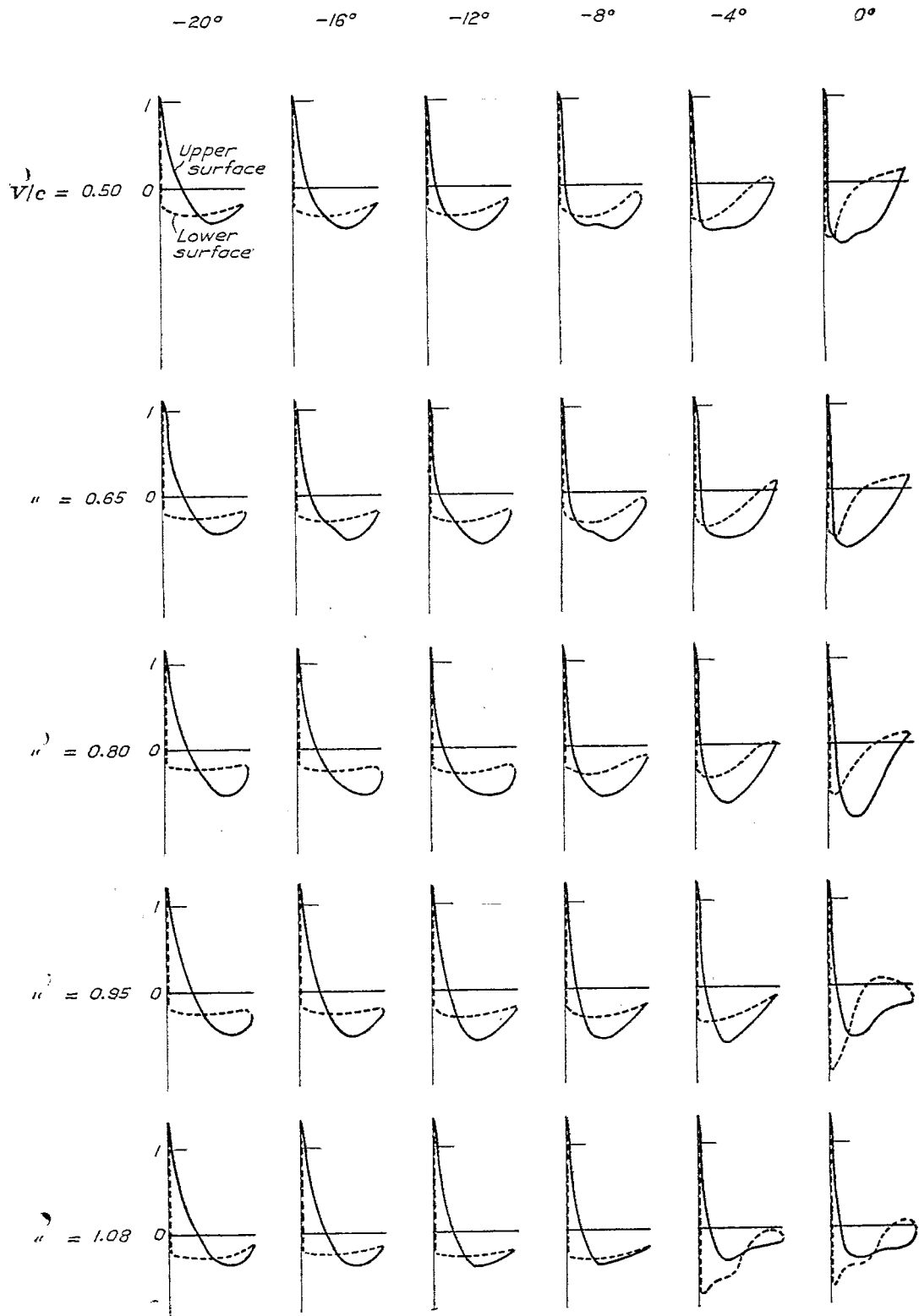


FIG. 5.—Continued



Airfoil 3

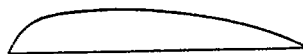
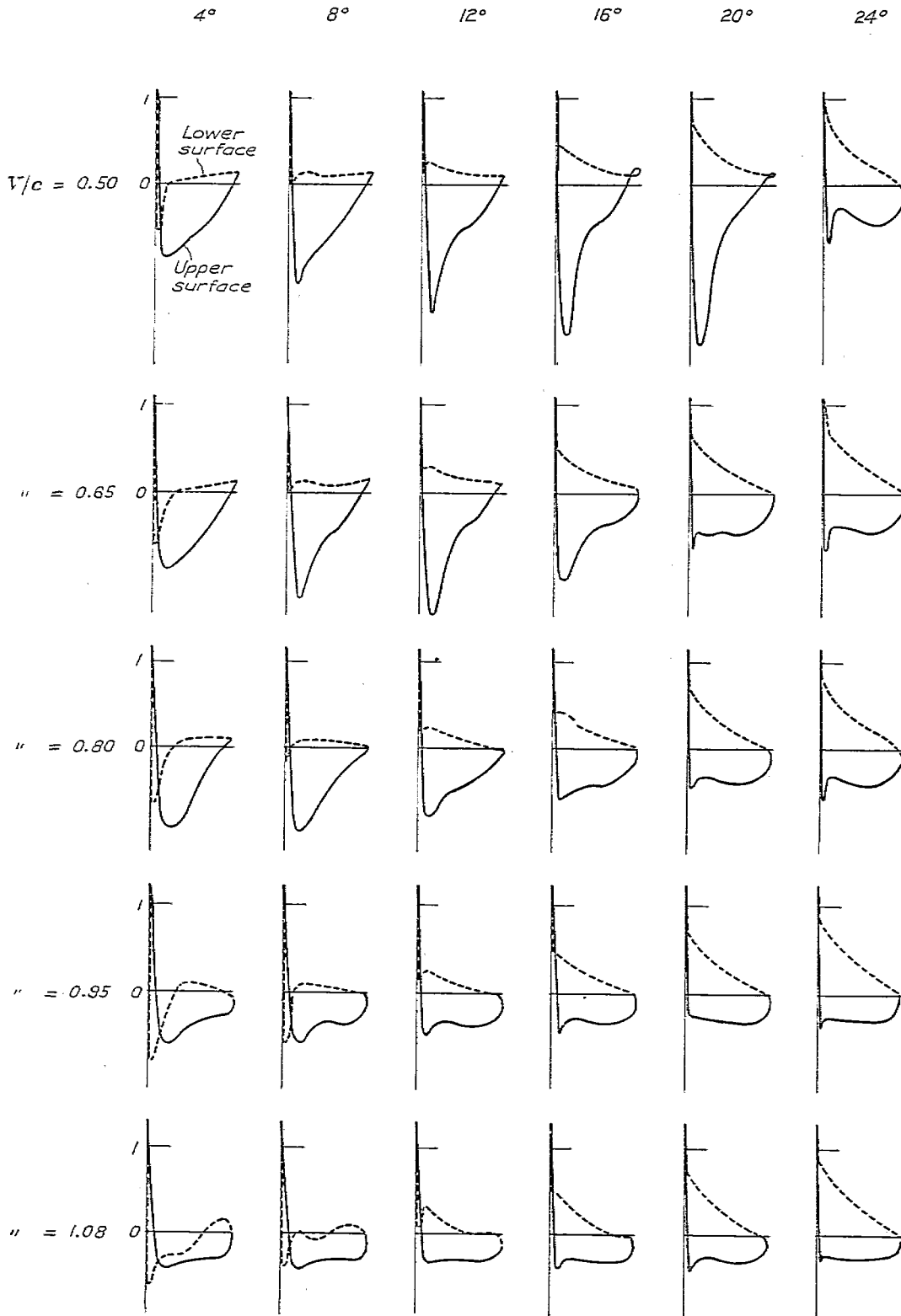


Fig. 6.—Distribution of pressure over airfoil 3 at various speeds and angles. Abscissae are distances from the nose measured along the chord. Ordinates are values of  $\frac{p-p_0}{\frac{1}{2}\rho V^2}$ .



Airfoil 3

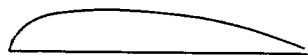


Fig. 6.—Continued

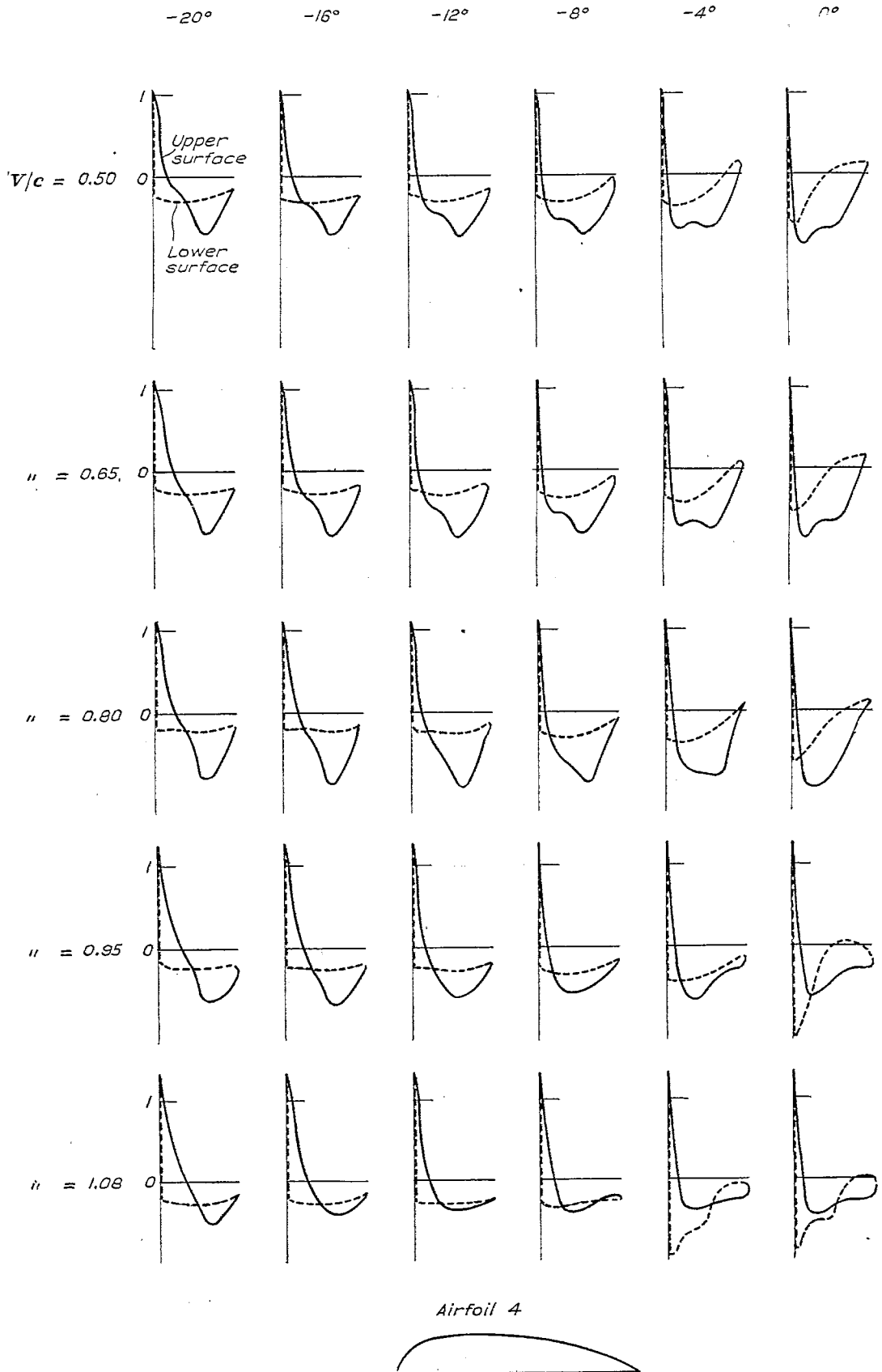
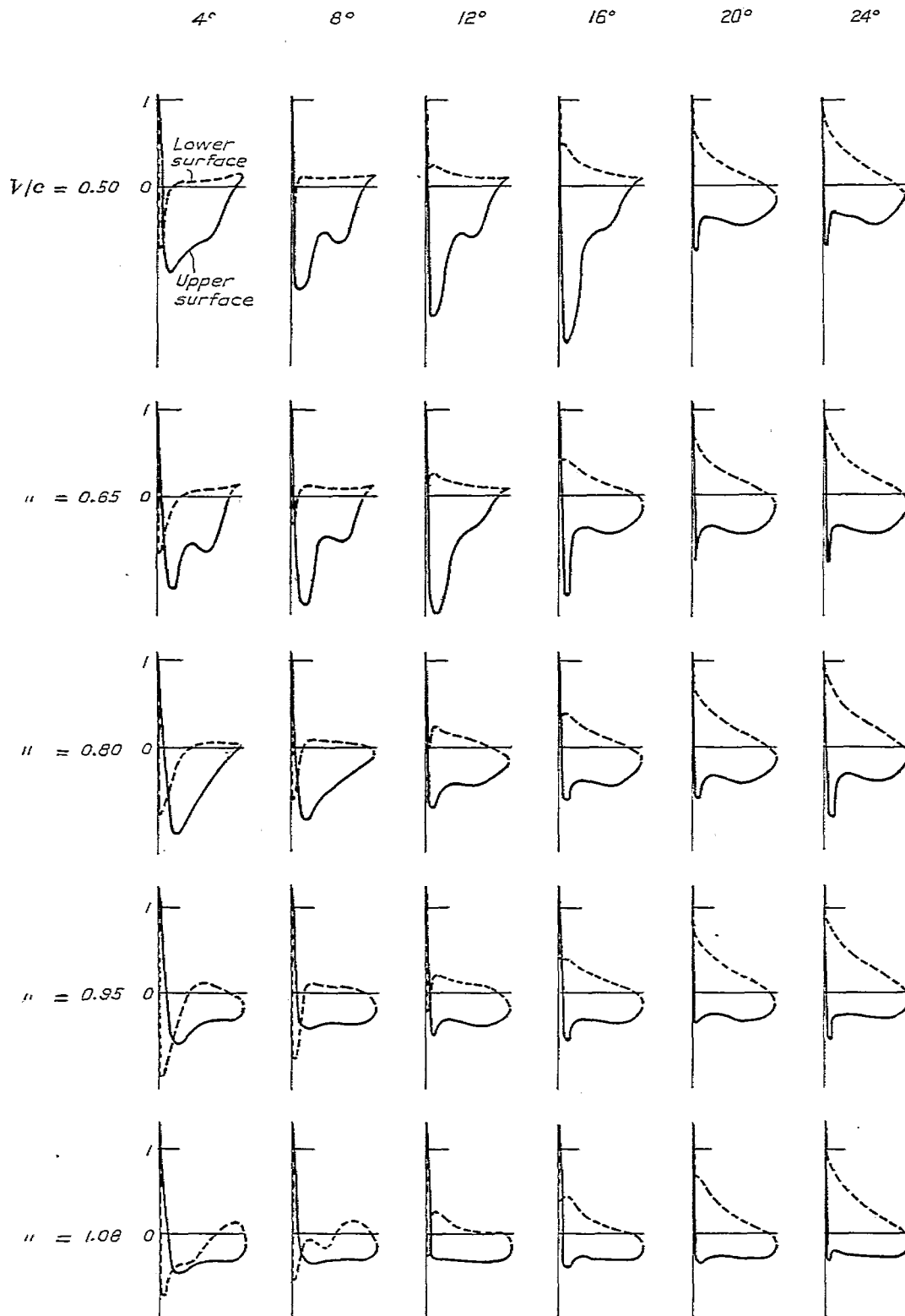


Fig. 7.—Distribution of pressure over airfoil 4 at various speeds and angles. Abscissae are distances from the nose measured along the chord. Ordinates are values of  $\frac{p-p_0}{\frac{1}{2}\rho V^2}$



Airfoil 4

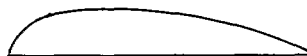


FIG. 7.—Continued

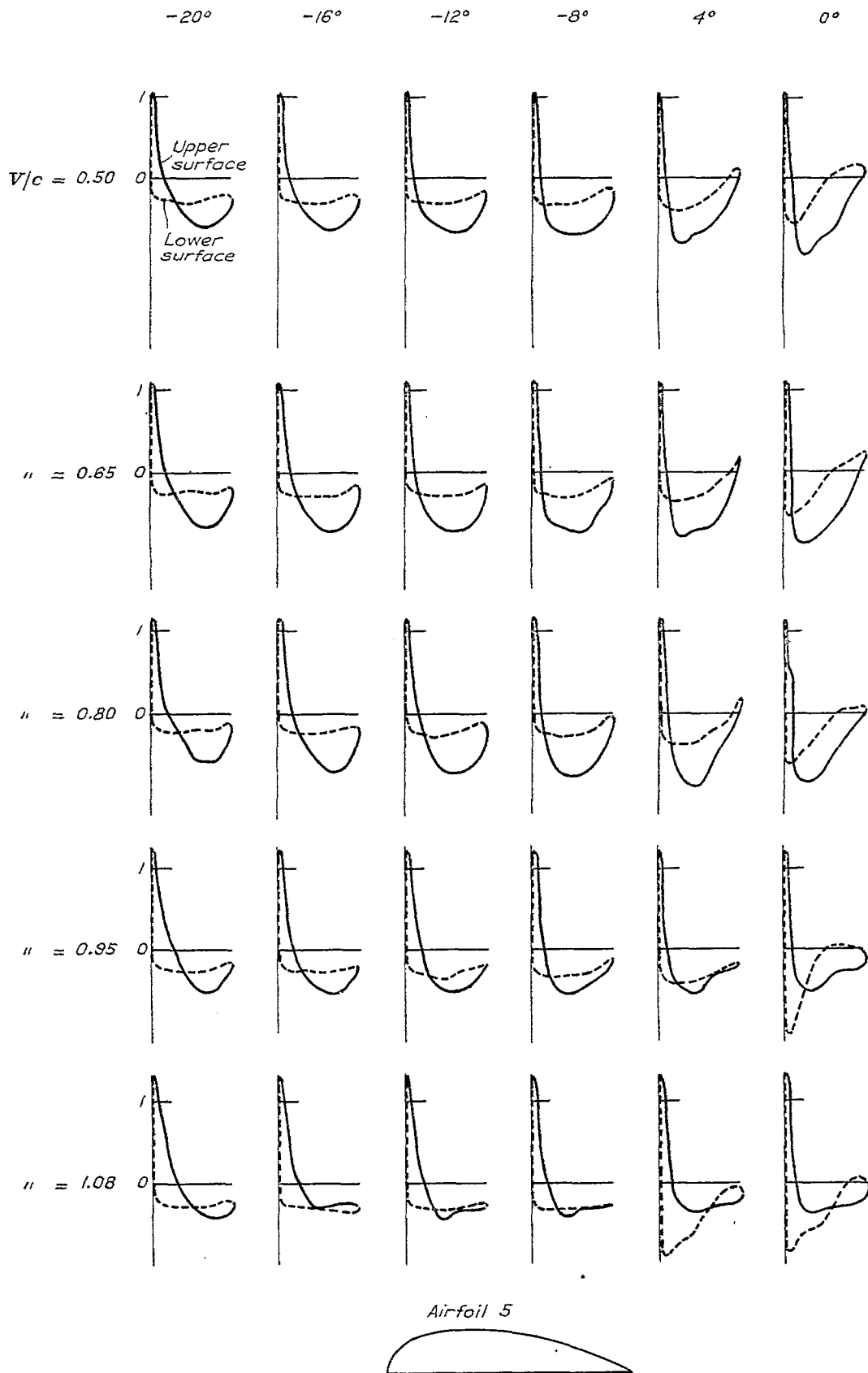


Fig. 8.—Distribution of pressure over airfoil 5 at various speeds and angles. Abcissae are distances from the nose measured along the chord. Ordinates are values of  $\frac{p-p_0}{\frac{1}{2}\rho V^2}$

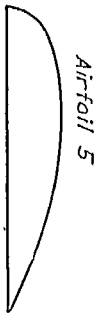
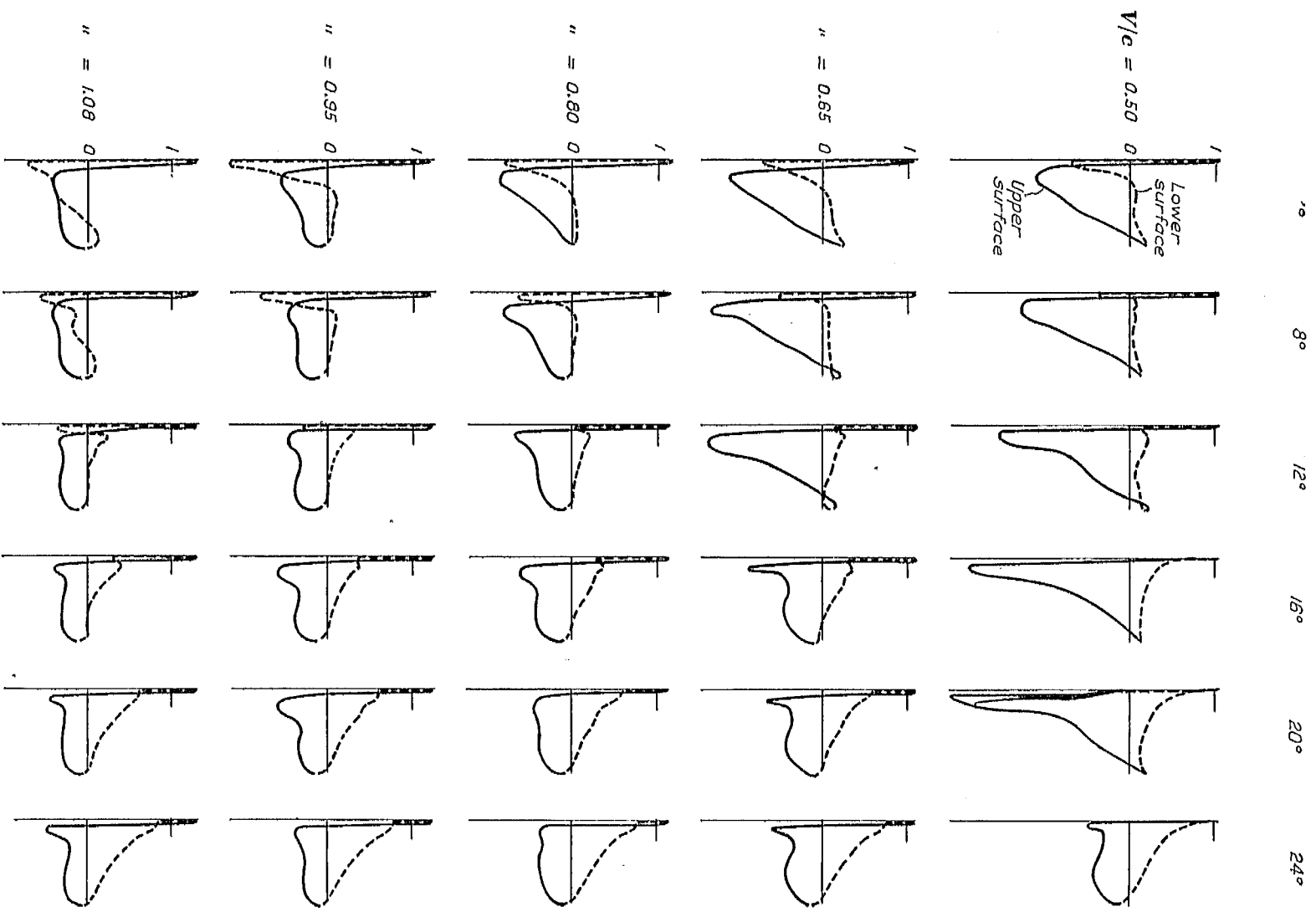


Fig. 8.—Continued

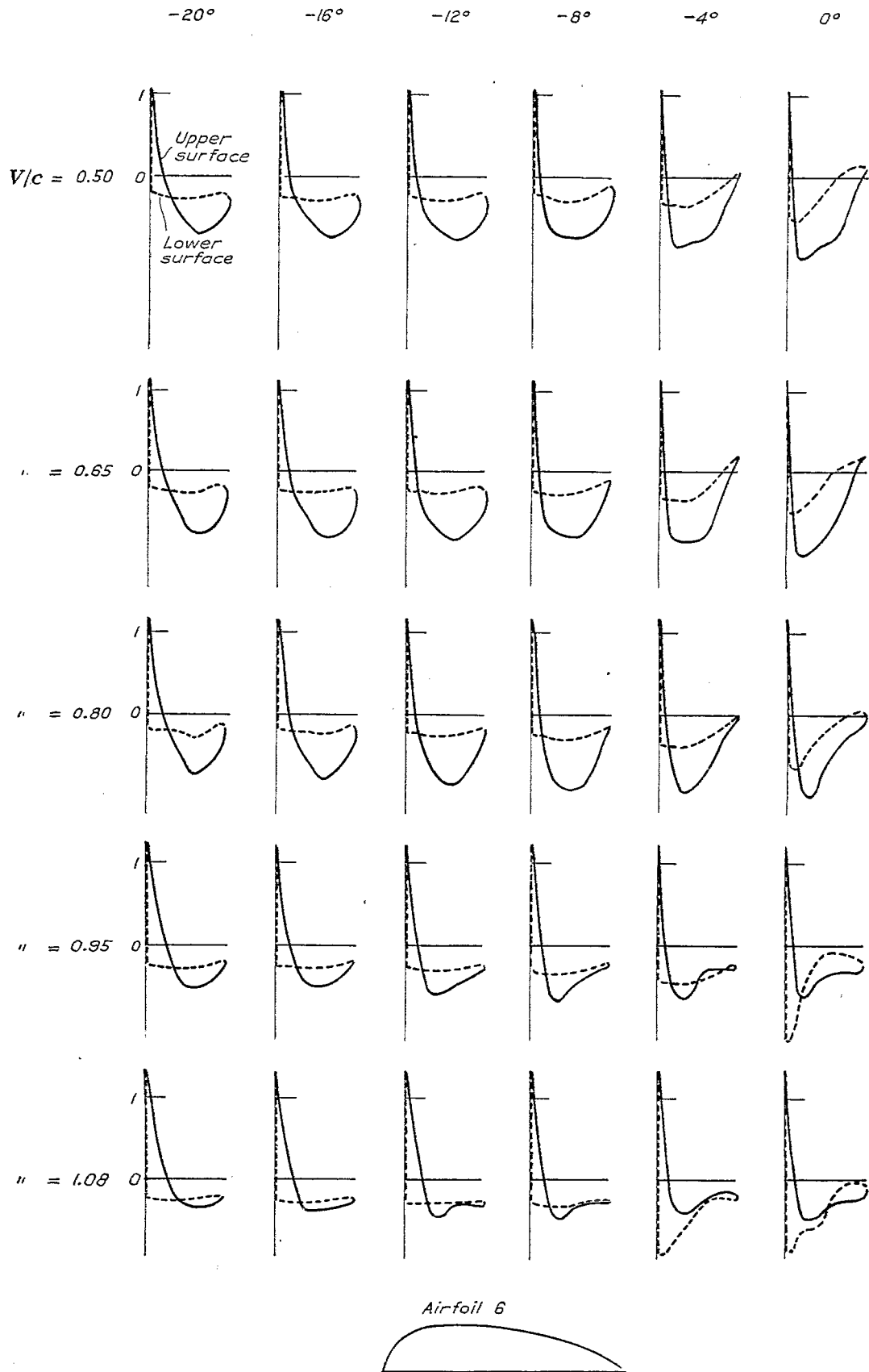


FIG. 9.—Distribution of pressure over airfoil 6 at various speeds and angles. Abscissae are distances from the nose measured along the chord. Ordinates are values of  $\frac{p-p_0}{\frac{1}{2}\rho V^2}$

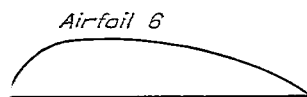
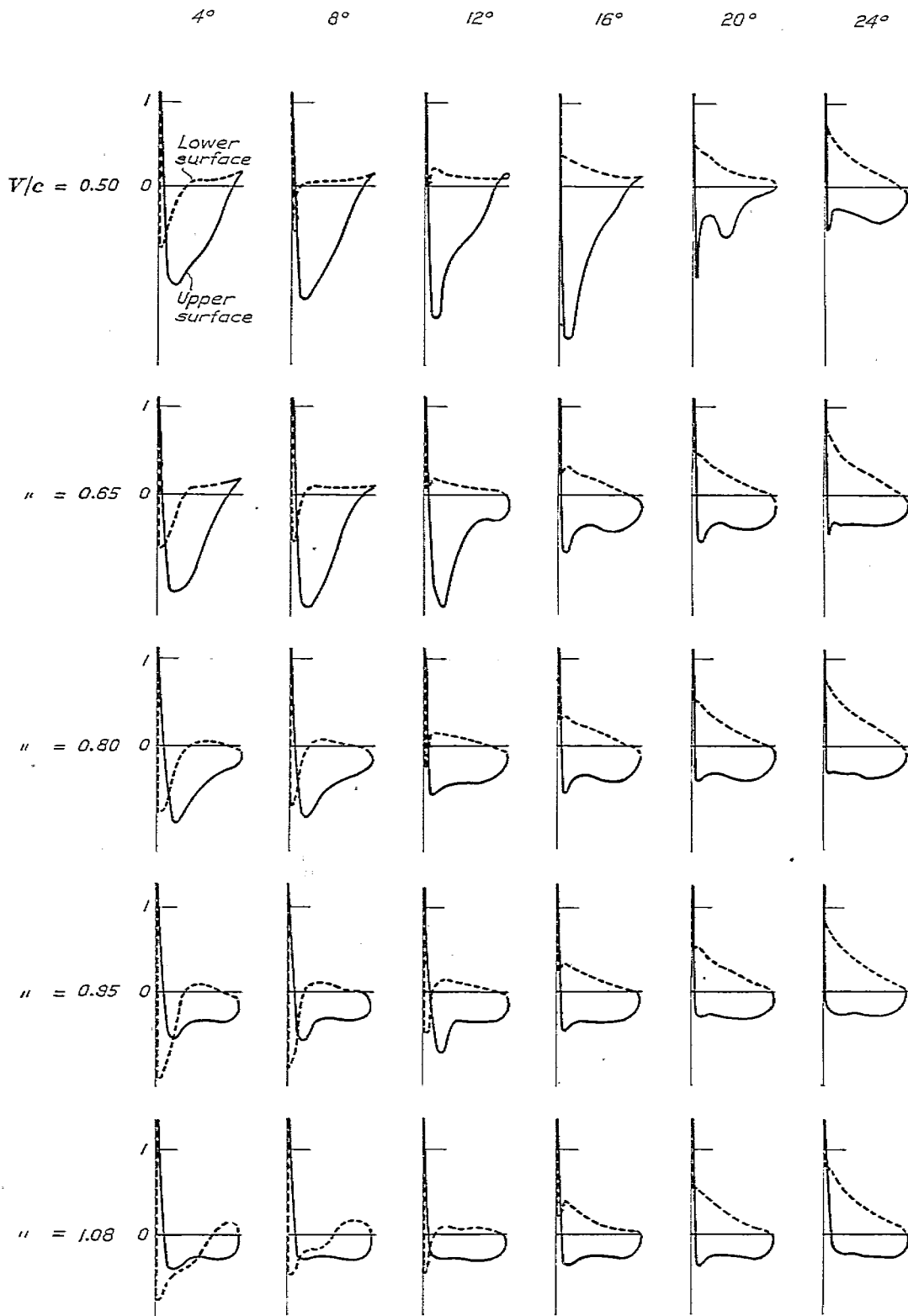


FIG. 9.—Continued

as abscissae and the second in which the ordinates are the same but the abscissae are distances perpendicular to the chord. The proof of this statement is obvious from Figure 10. The curves are of course determined by the values of the ordinates at a few discrete values of the abscissae. The usual method of finding the area is a graphical one of drawing in a faired curve and measuring the area with a planimeter or by counting small squares on coordinate paper. In the present case because of the large number of observations to be treated, a numerical method was found more satisfactory since it was much quicker and gave results which were more directly comparable.<sup>2</sup>

In the integration for the tangential force coefficient it was found desirable to interpolate additional pressure values at the ends since no stations could be placed close to the leading and trailing edge. Table III gives the factors for airfoil 1 of 0.10 camber ratio. The normal

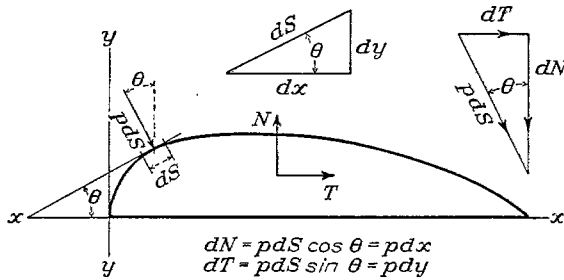


Fig. 10.—Diagram showing method of computing normal and tangential forces from the observed pressures

force factors are the same for all airfoils but the tangential force factors are proportional to the thickness of the airfoil, those for airfoil 2 being 1.2 times those for airfoil 1 and so on. It will be noted that the signs for the upper surface in the case of the normal force factors and for the rear of the upper surface in the case of the tangential force factors are negative, because a positive pressure acting on those parts of the airfoil produces negative forces, the normal force being called positive when directed from the

lower surface to the upper and the tangential force being called positive when directed from leading to trailing edge. The lower surface does not contribute to the tangential force since it is flat.

TABLE III

Station	Factors for normal force coefficient for all airfoils	Factors for tangential force coefficient for airfoil 1 only
Interpolated station at leading edge		0.0154
1	-.0476	.0464
2	-.0119	-.0003
3	-.0706	.0330
4	-.1684	-.0056
5	-.2251	-.0085
6	-.1500	-.0180
7	-.3264	-.0580
Interpolated station at trailing edge		-.0155
8	.0952	0
9	.0289	0
10	.1744	0
11	.2251	0
12	.1500	0
13	.3264	0

The values of the lift and drag coefficients obtained are shown in Figures 11 and 12 and in the tables in the appendix.

The moments about the leading edge and the positions of the center of pressure were computed by an approximate method. The approximation consisted first in the neglect of the moments of the components of the pressure parallel to the chord and second in the use of factors obtained by multiplying the normal force factor for a given station by the distance of the station from the nose. The errors arising from this procedure will be discussed in the section on "Accuracy."

The values of the approximate moment coefficients and center of pressure positions are given in the appendix and in Figures 13 and 14.

<sup>2</sup> Many such numerical methods of integration are described in textbooks on applied mathematics. In the present case a curve of the third degree was passed through four adjacent points, the ordinates being denoted by letters and the numerical values of the abscissae inserted. The area between the two inner ordinates, the curve, and the axis of abscissae was found by integration. At the end intervals special treatment was necessary and in general the procedure followed was to pass a curve of the second degree through the three end points and to integrate from the second point to the end of the airfoil. When this procedure is carried out and the results for all intervals added, there results a series of factors by which each ordinate is to be multiplied and the results of the multiplication summed for all stations to obtain the area.

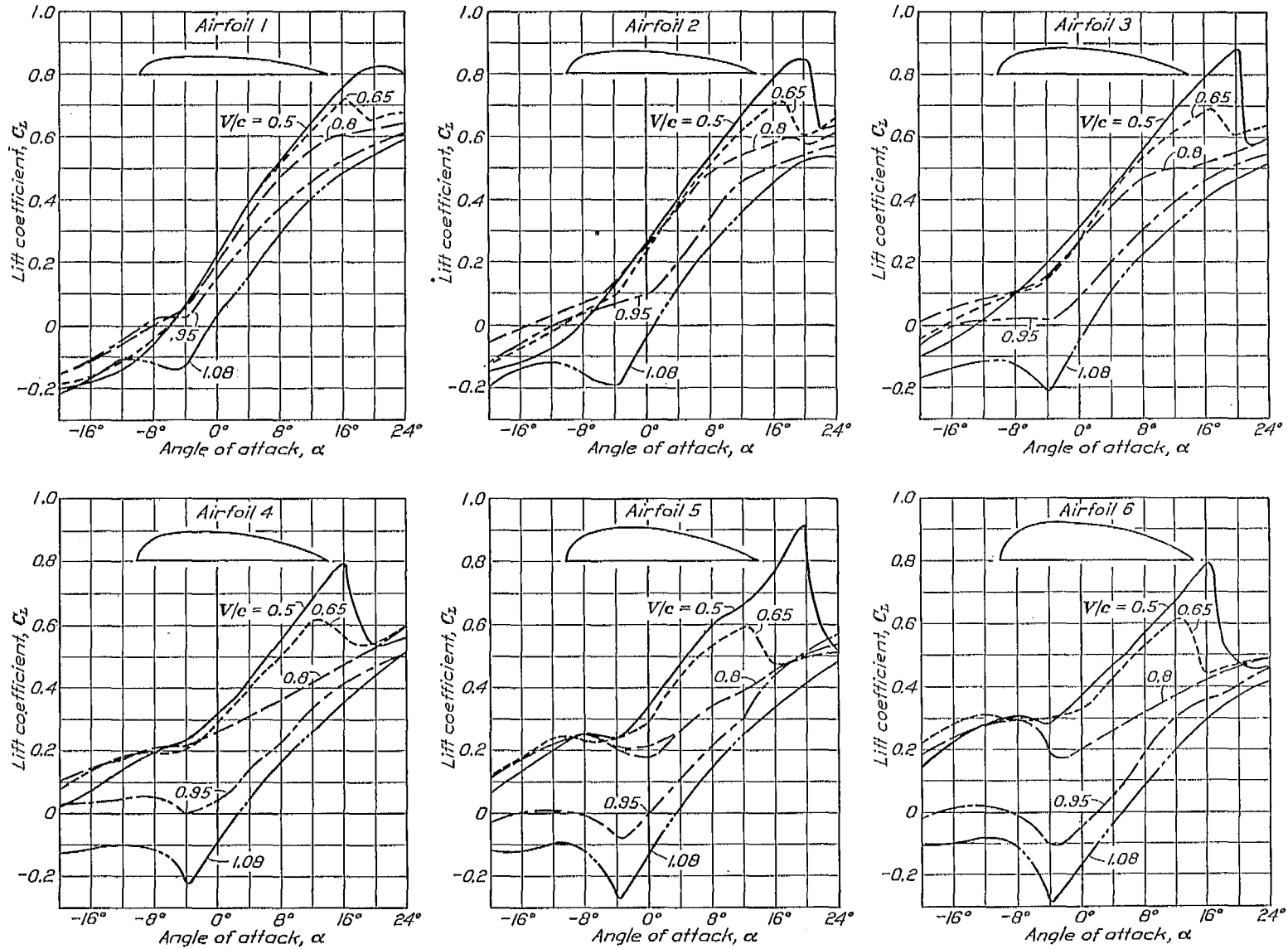


FIG. 11.—Lift coefficients for the six airfoils at various speeds and angles. Numbers on the curves denote values of  $V/c$

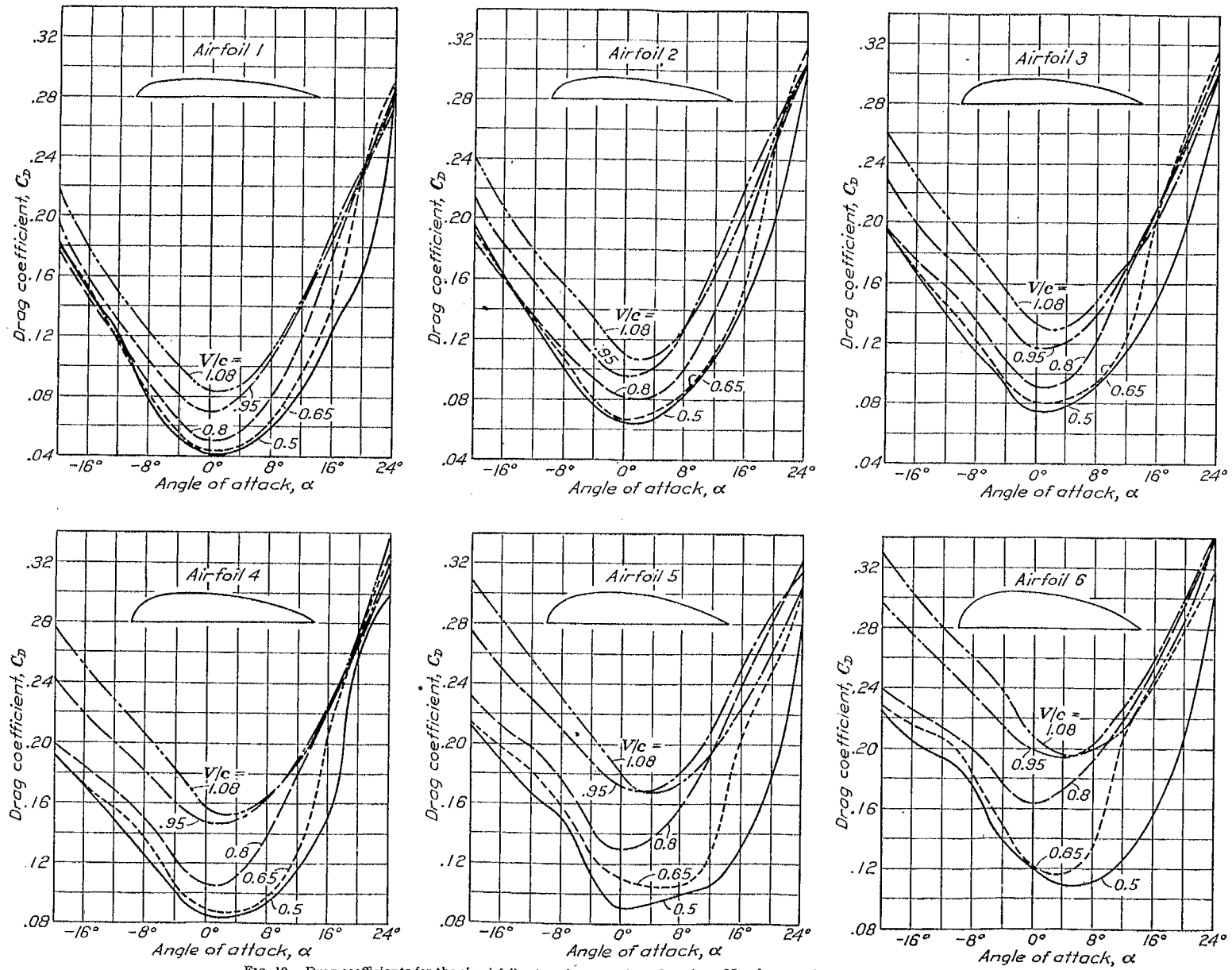


FIG. 12.—Drag coefficients for the six airfoils at various speeds and angles. Numbers on the curves denote values of  $V/c$

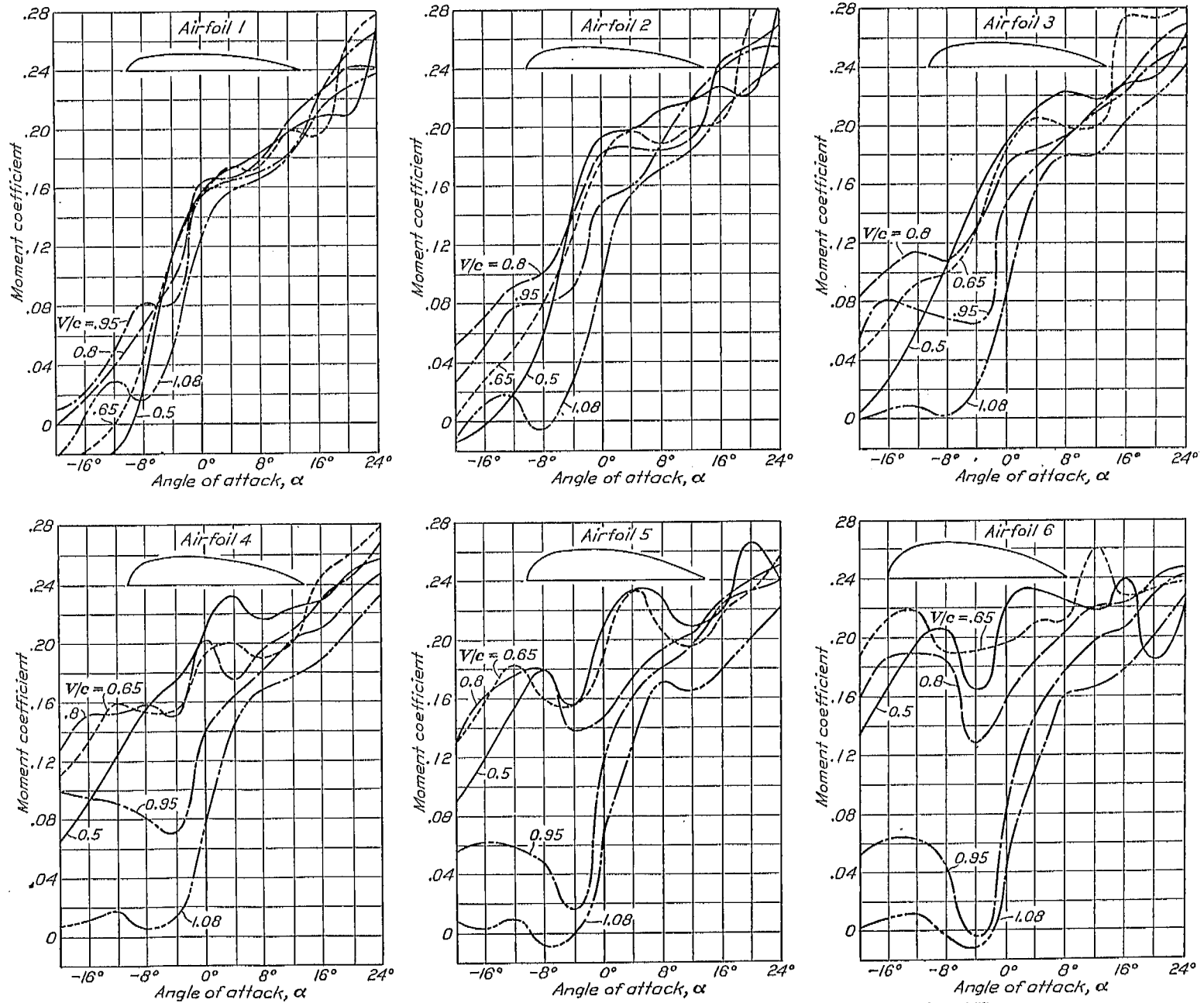


FIG. 13.—Moment coefficients for the six airfoils at various speeds and angles. Numbers on the curves denote values of  $V/c$

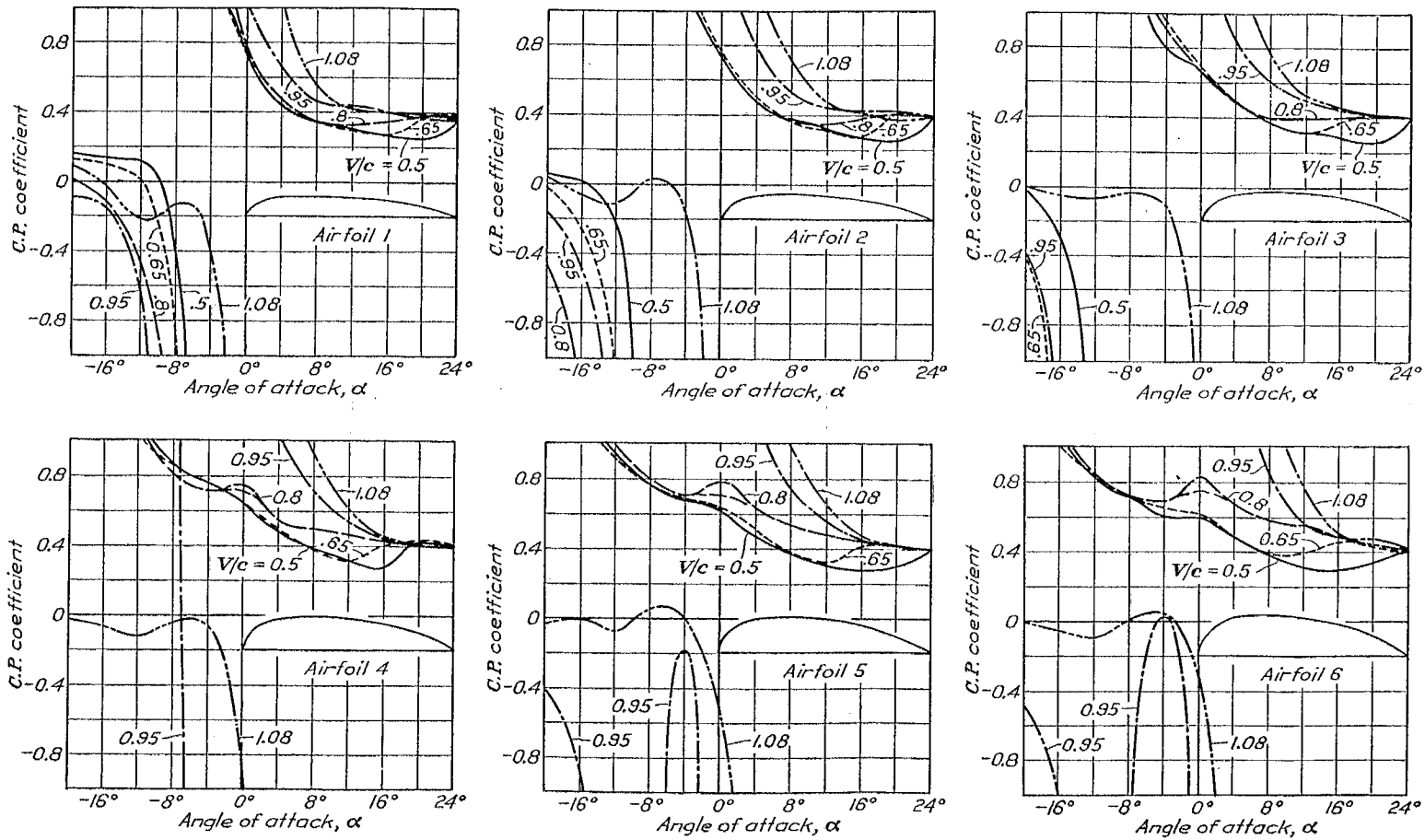


FIG. 14.—Center of pressure coefficients for the six airfoils at various speeds and angles. Numbers on the curves denote values of  $V/c$

## EFFECTS OF POSITION OF AIRFOIL IN AIR STREAM AND OF THE SIZE OF THE AIR STREAM

A number of auxiliary measurements were made in order to find the effects of variations in the experimental conditions as regards the position of the model in the air stream and the size of the air stream. The complete series of tests was carried out with the center of the airfoil at a height of 4 inches above the plane of the orifice mouth in air streams of approximately 2 inches in diameter. The measurements on airfoil 3 were repeated for a number of stations at speeds of 0.8 and 0.95 times the speed of sound at a distance of 2 inches above the plane of the orifice mouth. Typical curves are shown in Figure 15. It will be noted that in general the agreement is very good, the greatest difference being near  $0^\circ$  for station 8 at 0.8 speed where the curves for the two heights are shifted with respect to each other. The effect is less marked for the same station at 0.95 speed. In fact the flow around airfoil 3 at 0.8 speed at negative angles is rather unstable and in one instance (not shown) a somewhat larger difference was found at large negative angles. In general we may say that a change in the height of the airfoil above the orifice does not change the pressure distribution to any marked extent except in those cases where the flow is unstable.

Table IV shows the good agreement between results obtained with the airfoil in its normal position and those obtained with the airfoil reversed and turned through an equal angle in the opposite direction. The differences are so small that they can not be readily shown on the scale used in Figure 15.

TABLE IV  
AIRFOIL 3.— $V/c=0.5$ . RATIO OF PRESSURES TO VELOCITY PRESSURE,  $\frac{1}{2}\rho V^2$

Angle	Station 2		Station 6	
	Normal	Reversed	Normal	Reversed
$-20^\circ$	0.895	0.904	-0.428	-0.421
$-16^\circ$	.794	.806	-.481	-.479
$-12^\circ$	.664	.676	-.514	-.517
$-8^\circ$	.514	.522	-.525	-.524
$-4^\circ$	.353	.362	-.510	-.520
$0^\circ$	.179	.188	-.516	-.520
$4^\circ$	-.059	-.034	-.489	-.500
$8^\circ$	-.363	-.339	-.469	-.475
$12^\circ$	-.721	-.698	-.440	-.449
$16^\circ$	-1.107	-1.088	-.379	-.389
$20^\circ$	-1.502	-1.508	-.272	-.278
$24^\circ$	-.673	-.681	-.464	-.452

A few measurements were made with a smaller orifice, 1.2 inches in diameter. As would be expected, a large effect was found because of the decrease in aspect ratio. The most striking feature of the results in the case of the smaller air stream was the marked drop in the values of the pressure decrease on the top surface. The pressures on the lower surface were not affected as much but the relations could not be expressed in any simple way.

## ACCURACY

*Pressure distribution.*—The precision of the pressure measurements was satisfactory as illustrated by the results in Table IV, the differences occurring between the normal and reversed positions being typical of differences between repeat measurements. The operating conditions were very steady and required only occasional slight adjustments of the pressure. On the average the curves could certainly be repeated to within 1 per cent of the pipe pressure or one-twentieth of a degree where the change with angle was very great.

The application of the results to other conditions requires a consideration of other factors, the most important of which is the effect of aspect ratio. This effect is a very large one, and experimental data are still lacking to make quantitative estimates. The information available, so far as the total forces are concerned, will be summarized in the section on "Discussion and Comparison with Earlier Work." No method is as yet known for computing the effect of aspect ratio on pressure distribution, even at ordinary wind-tunnel speeds and for larger aspect ratios.

*Integration of pressures.*—A discussion of the precision and accuracy of the lift and drag coefficients derived from pressure measurements introduces several new considerations. It has been pointed out that the values would not be expected to agree with the forces obtained by direct measurement because of the absence of the skin friction in the pressure integration. This effect would be most pronounced in the drag coefficients which would accordingly be somewhat too low. In addition to this, it must be remembered that the pressure distribution was taken at the mid-section so that the results of the integration do not apply to an airfoil spanning the stream but to a single section only. These two factors should be studied by making force measurements on the same airfoils, and it is hoped that this can be done at a later date.

There still remains a final consideration, namely, as to the accuracy with which the resultant action of the pressure distribution has been computed from the pressures at 13 stations. It is,

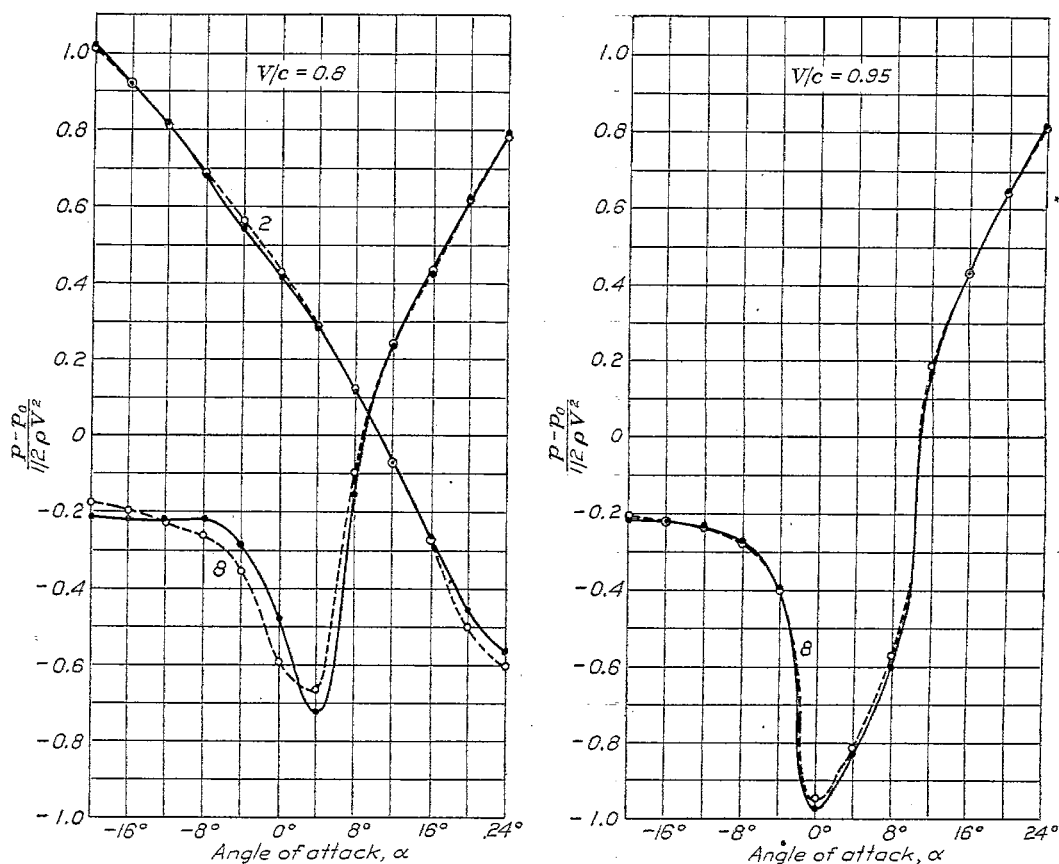


FIG. 15.—Comparison of measurements on airfoil 3 at 2 inches (solid curve) and 4 inches (dotted curve) above the plane of the orifice mouth. Numbers on curves denote stations

of course, impossible, strictly speaking, to estimate this accuracy without measuring the pressure at a very large number of stations, since we have no *a priori* knowledge of the form of the pressure-distribution curves. We can therefore only express an opinion as to the probable accuracy. To obtain a reasonable basis for this opinion we have followed the older method of drawing in curves connecting the points in a reasonable way for a number of cases, and have compared the values of the coefficients obtained by the use of a planimeter with those obtained by the numerical method. Table V shows typical results. The average difference without regard to sign is 0.01, which may be taken as a measure of the precision of the normal force coefficients.

The tangential force coefficients are subject to a somewhat greater error because of the absence of stations near the leading and trailing edges. It is estimated that the values given are within 0.03 of the values that would have been obtained if it had been possible to use a larger number of stations. The comparative values are probably correct within 0.01 to 0.02 as judged by the smoothness of the results. From this it follows that the drag coefficients are correct within about the same limits.

The moment coefficients were computed by an approximate method described in the section on integration of pressures. The exact method was used for a few cases and found to give moment coefficient values differing by 0.007 from the approximate values, and center of pressure positions (in the flatter portions of the curve) differing by 0.02. It was not believed profitable to carry through the exact computations in all cases because the time required would have been very great and the chief interest is in relative rather than absolute values.

TABLE V  
COMPARISON OF NORMAL FORCE COEFFICIENTS BY GRAPHICAL AND NUMERICAL METHODS

Angle	Airfoil 6, $V/c=0.5$		Airfoil 6, $V/c=1.08$	
	Graphical method	Numerical method	Graphical method	Numerical method
-20°	0.060	0.064	-0.218	-0.210
-16°	.145	.153	-.177	-.168
-12°	.232	.238	-.129	-.132
-8°	.275	.289	-.146	-.137
-4°	.280	.274	-.276	-.278
0°	.367	.371	-.150 to -.191	-.133 to -.171
4°	.482	.476	-.050	-.025
8°	.611	.595	.116	.125
12°	.688	.680	.221	.221
16°	.803	.811	.358	.360
20°	.499	.524	.442	.455
24°	.558	.552	.516	.528

#### OBSERVATIONS OF FLOW NEAR THE AIRFOILS

A description was given in Report No. 207 of the National Advisory Committee for Aeronautics of the behavior of an oil film on the surface of an airfoil at high speeds. Some additional observations were made at Edgewood and Figures 16 and 17 illustrate the type of pattern

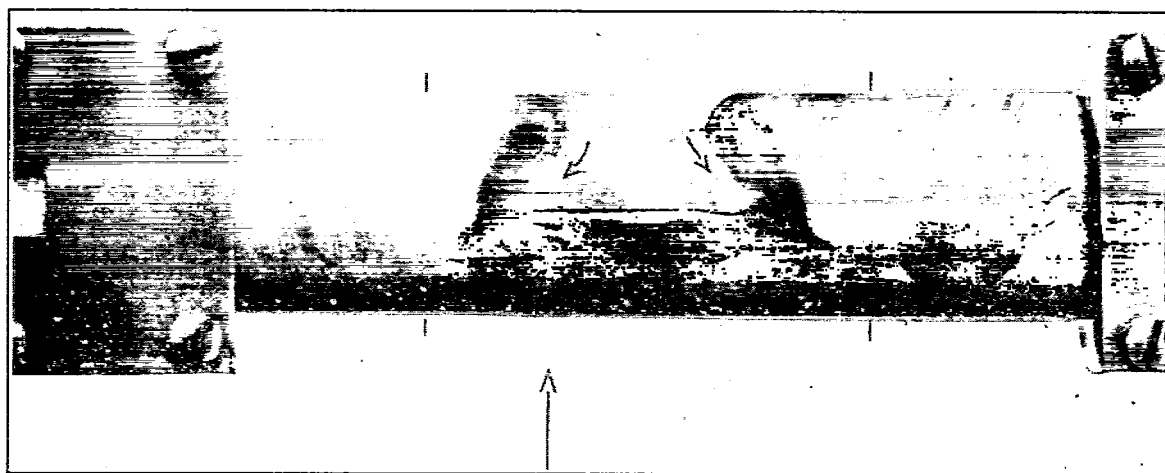


FIG. 16.—Oil flow pattern on the upper surface of airfoil 1 at 0° angle of attack,  $V/c=1.08$ . The flow of the air stream is toward the top of the page. Note the separation from the surface shown by the ridge of stationary oil at about 0.43 the chord length from the leading edge. The diameter of the orifice is twice the chord length of the airfoil

formed. The technique of observing flow near a surface by oil films has been developed at McCook Field and elsewhere. The photograph in Figure 16 shows a film of oil and lampblack on the upper surface of airfoil 1 at 0° to the wind at a speed of 1.08 times the speed of sound. Figure 17 shows airfoil 6 under the same conditions. The flow over the greater part of the upper surface is in a direction opposite to the general direction of the stream and the air moves off in the familiar tip eddies whose traces are shown at the boundary of the air stream. It appears that the region of low pressure is broken down by a flow about the trailing edge from the lower surface and that there is a separation of the main stream from the upper surface.

Time was not available to study this phenomenon in detail at Edgewood, but further observations of a similar qualitative nature were made in a 1.2-inch jet at the Bureau of Stand-

ards at a speed of 0.65 times the speed of sound. It appears that flow around the trailing edge does not occur in all cases, but that there may be a region of reverse flow and eddy formation over a limited area on the upper surface. In the case of the thin airfoils the disturbance begins as the angle to the wind is increased, in the region just behind the maximum ordinate, whereas with the thickest airfoil of 0.20 camber ratio it begins at the trailing edge. With the airfoil of 0.18 camber ratio the disturbance begins nearly simultaneously at both places.

Flow of oil mixtures of this type depends on gravity, viscosity, surface tension, adhesion, and other factors and the question was raised as to whether the oil flow corresponded to the air flow or merely to differences in pressure. An attempt was made to answer this by feeding threads through the tubing inserted in the airfoil so as to project from the airfoil through the pressure hole. (The threads were readily drawn through by a suction pump.) The threads indicated the same direction of flow as the oil on the surface. As a further check, a small exploring tube with projecting thread was constructed to explore the regions at greater distances from the airfoil. It was found that the presence of the exploring tube changed the oil flow to some extent. Nevertheless it appeared that the layer of reverse flow is extremely thin at its initial appearance but becomes thicker as the angle is increased until it is a millimeter or more in thickness.

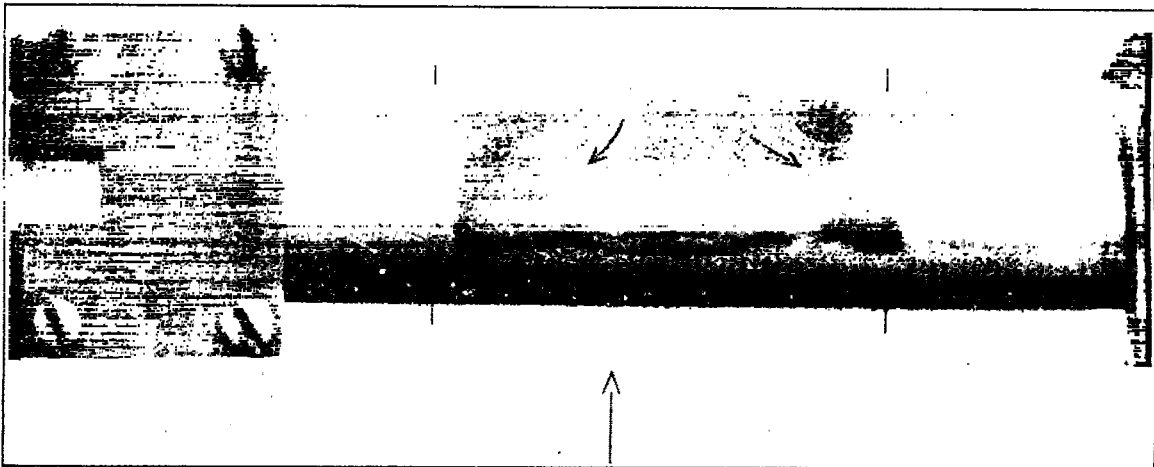


FIG. 17.—Oil flow pattern on the upper surface of airfoil 6 at  $0^\circ$  angle of attack,  $V/c=1.08$ . The flow of the air stream is toward the top of the page. Note the separation from the surface shown by the ridge of stationary oil at about 0.29 the chord length from the leading edge. The diameter of the orifice is twice the chord length of the airfoil

A change in flow thus begins in a fairly sudden manner in the boundary layer on the upper surface immediately behind the maximum ordinate for thin airfoils at the lower speeds, and at the trailing edge for thick airfoils at the lower speeds. At the lower speeds the change takes place at comparatively large angles and is analogous to the well known burble point. At the higher speeds the change takes place at small angles and is accompanied by a rapid decrease in lift coefficient and increase in drag coefficient.

At  $V/c=1.08$  standing compressional waves (bow waves) were observed at a distance of about 0.5 inch in front of the leading edges of the airfoils.

#### DISCUSSION AND COMPARISON WITH EARLIER WORK

A careful inspection of the pressure distribution curves, Figures 4 to 9, shows the existence of regions characteristic of flow of the type described in which there is a separation from the surface. For example in Figure 6 for airfoil 3 the distribution over the upper surface for a speed of  $0.5c$  at  $24^\circ$ , shows a sharply defined peak followed by a region of nearly constant decrease in pressure such as is found in the case of a cylinder or sphere where the flow breaks away from the surface. A similar distribution may be observed at  $0.65c$  at  $20^\circ$  and  $24^\circ$ ,  $0.8c$  at  $16^\circ$ ,  $20^\circ$ , and  $24^\circ$ ,  $0.95c$  at  $4^\circ$ ,  $8^\circ$ ,  $12^\circ$ ,  $16^\circ$ ,  $20^\circ$ , and  $24^\circ$ , and  $1.08c$  at all positive angles. In fact it is possible to trace a rough locus of speeds and angles at which the change takes place. The steps in speed and in angles are unfortunately so far apart that the exact position can not be plotted, but it

may be seen that for thick airfoils at a given speed the break occurs at lower angles and at a given angle at lower speeds than for the thin airfoils. The location of the change in flow is facilitated by the fact that for the burbling type of flow the pressure at the trailing edge is lower than the static pressure whereas for the smooth high lift type it is higher than the static pressure.

It must be remembered that no trace of the break can be detected in the pressure distribution until the flow is changed at one of the stations at which observations were made, so that the break in the pressure distribution as given appears less sharp than it really is. It seems evident, from the visual observation of the oil flow, that the change in flow takes place suddenly, but that it is confined to a small area at first and spreads rapidly as the speed or angle is increased. The evidence of beginning in a small region near the maximum ordinate in the case of the thin airfoils is not entirely clear from the pressure distribution curves alone, although indications may be observed, especially in the case of airfoil 4. In the case of airfoil 1 between  $16^\circ$  and  $20^\circ$  the oil flow experiments show that the reverse flow begins and spreads beyond the last station for pressure measurements, so that only in exceptional cases can the origin be traced on pressure distributions taken at intervals of  $4^\circ$ . The spreading is even more rapid for airfoil 6.

These rapid changes of flow are reflected in the lift coefficient curves (fig. 11) with a still greater reduction in the sharpness of the break. The sudden burble points are very noticeable in most cases for speeds of  $0.5c$  and  $0.65c$ . For the thin airfoils there is a rapid change in the lift coefficient with speed between  $0.8c$  and  $0.95c$  for all the lower angles. Similar changes occur between  $0.65c$  and  $0.8c$  for the thick airfoils.

These curves give in a more systematic manner than was possible in Report No. 207 the variation of lift coefficient with speed at all angles from  $-20^\circ$  to  $+24^\circ$ . The same shift of the angle of no lift first to high negative angles and then to  $0^\circ$  or a small positive angle is shown in more detail. The increase in lift coefficient at large negative angles, followed by a rapid decrease as the speed is increased, is traced to negative lift coefficients. The changes between 0.5 and 1.08 times the speed of sound increase with increasing thickness, and there is every reason to believe that the same decrease may be expected for airfoils of smaller camber than 0.10 at higher speeds. The minima in all curves at high speeds and in the curves for the thicker airfoils at low speeds are associated with the large suction on the lower surface near the leading edge which develops near  $0^\circ$ . It is probable that this effect would not be present with a more rounded leading edge or on a doubly cambered section.

A comparison of the lift coefficient curves with those given in Report 207 will show that the Edgewood values are lower, as would be expected from the lower aspect ratios. The results can not be directly compared, since the Edgewood values apply only to the mid-section, and the form of the lift distribution curve along the span is not known for these speeds.

The rapid change in the lift coefficient in the Edgewood experiments occurred at a value of  $V/c$  about 10 per cent greater than at Lynn. The chord length used at Edgewood was one-third that used in the Lynn measurements. Therefore the Reynolds Number at which the rapid change in the lift coefficient took place at Edgewood was only about one-third that at Lynn. The change in the lift coefficient appears therefore to be much more definitely associated with  $V/c$  than with  $\rho V l / \mu$ . In other words, the compressibility effect is predominant.

There are two possible explanations for the somewhat larger value of  $V/c$  at which the rapid change in the lift coefficient occurred in the Edgewood experiments. First, the Reynolds Number may still have some effect. Second, a possible aspect ratio effect. For example, photographs taken in the 1.2-inch jet indicate that the change in flow takes place at a greater angle of attack than in the 2-inch jet for airfoil 6 and at approximately the same angle for airfoil 1. Moreover at ordinary wind tunnel speeds the burble point occurs at a greater angle of attack for the smaller aspect ratio. Hence it is possible that the exact angles and speeds at which a change in flow takes place vary with the aspect ratio.

When we come to drag coefficients there is a somewhat different state of affairs. We should expect the drag coefficient computed from the pressure integration to be lower than the true drag coefficient because of skin friction. We might also expect the coefficient for a section near

the center to be somewhat lower than the average for the whole section. Hence it is probable that the total drag coefficient for the whole section is greater by some unknown amount than that computed from the pressure distribution. However, the values computed from the pressure integration at Edgewood are very much higher than those obtained at Lynn at angles near  $0^\circ$ . We should expect the drag coefficient for the whole section to be somewhat higher than the Lynn values owing to the smaller aspect ratio, but the difference is too great to be attributed entirely to an aspect ratio effect. It seems highly probable that there is a comparatively large effect of Reynolds Number on drag coefficient even at these high speeds. We hope to obtain more definite information on this point in later tests.

The drag coefficient curves given in Report 207, Figures 16 to 21, show a rapid rise in coefficient for angles near  $0^\circ$ , as, for example, Figures 21 for airfoil 6. The maximum speeds reached in most cases were between 0.8 and 0.95 the speed of sound. The Edgewood tests (fig. 12) show that this rapid increase is followed by a region of nearly constant coefficient, and in fact there is some indication of this in a few observations in Report 207. In other words, the drag curves are probably somewhat similar to the well-known Gavre curve for projectiles.

The center of pressure curves (fig. 14) give a more detailed picture of the backward motion at the usual working angles. These require little discussion, since they merely reflect the more even distribution of load at the higher speeds. The behavior at negative angles corresponds to the zero lift positions, of which there are three in some cases.

The moment curves (fig. 13) show that the effect of the reduction in force coefficients is greater than the backward motion of the center of pressure, so that the moment coefficient is in general reduced by increase in speed at a constant angle.

There remains for discussion but one observed fact which is not represented in the coefficient curves. The actual value of the maximum decrease in pressure on the upper surface seems limited, the average observed maximum value for all speeds greater than 0.5 the speed of sound and for all airfoils being approximately 32 cm. of Hg. The largest single value of  $p_o - p$  observed was 37 cm. Hg. or  $p/p_o = 0.51$ . This ratio is not far from the critical ratio for air, namely 0.53, and this observation suggests that in an air stream in which the flow obeys the law of Bernouilli the pressure can not decrease indefinitely but reaches a limit as soon as the ratio of the pressure to the static pressure at a large distance in front of the body causing the pressure change reaches the critical value of 0.53. Lower pressures may be produced in "dead air" spaces where the flow leaves the surface of the body as on the lower surface of the airfoils near the leading edge. In this case the pressure decreased to about one-fourth of the atmospheric pressure.

#### CONCLUSIONS

The changes in the aerodynamic characteristics of airfoils at high speeds have been studied in detail by means of pressure distribution measurements and a more extensive and more systematic series of observations has been described. The conclusions of Report No. 207 have been verified and extended to higher speeds. Observations have been made of the air flow near the surface and correlated with the force measurements. Large changes have been shown to be associated with the sudden breaking away of the flow from the upper surface.

It has been shown that the variation in lift coefficients is due very largely to a compressibility effect, although the additional effect of viscosity can apparently still be traced in the drag coefficients.

#### ACKNOWLEDGMENTS

The authors wish to acknowledge their indebtedness to Messrs. W. H. A. Boyd and P. S. Murphy for assistance in connection with the measurements and to Messrs. G. C. Hill and J. L. Ewin for assistance in the reduction of the observations.

OBSERVED VALUES OF  $\frac{p-p_e}{q}$ , AIRFOIL 1

$V/c=0.50$

Station	Angle of attack											
	-20°	-16°	-12°	-8°	-4°	0°	4°	8°	12°	16°	20°	24°
1	1.051	1.012	0.934	0.815	0.696	0.534	0.263	-0.134	-0.637	-1.235	-1.895	-0.996
2	.786	.664	.506	.332	.144	-.061	-.348	-.718	-1.174	-1.659	-2.110	-.667
3	.414	.254	.071	-.109	-.307	-.515	-.771	-1.052	-1.325	-1.546	-1.784	-.576
4	.141	.008	-.131	-.271	-.397	-.528	-.662	-.798	-.985	-1.045	-.958	-.528
5	-.089	-.175	-.252	-.316	-.371	-.423	-.469	-.497	-.464	-.472	-.445	-.528
6	-.219	-.261	-.291	-.315	-.329	-.345	-.346	-.321	-.306	-.273	-.217	-.446
7	-.269	-.265	-.236	-.223	-.226	-.195	-.149	-.114	-.086	-.044	-.000	-.233
8	-.278	-.301	-.331	-.385	-.537	-.754	-.128	.183	.383	.576	.728	.798
9	-.284	-.308	-.333	-.391	-.519	-.587	.024	.185	.323	.479	.614	.672
10	-.305	-.328	-.357	-.394	-.475	-.210	.040	.133	.230	.349	.454	.508
11	-.322	-.346	-.369	-.384	-.275	.017	.036	.088	.149	.222	.290	.335
12	-.304	-.326	-.327	-.279	-.036	.042	.051	.082	.116	.158	.206	.232
13	-.233	-.241	-.207	-.088	.080	.082	.082	.087	.094	.114	.126	.061

$V/c=0.65$

1	1.086	1.047	0.980	0.874	0.762	0.595	0.374	0.079	-0.299	-0.706	-0.847	-0.864
2	.848	.715	.566	.396	.230	.073	-.263	-.584	-.931	-1.272	-.767	-.446
3	.470	.293	.107	-.092	-.255	-.467	-.743	-1.031	-1.328	-1.538	-.543	-.397
4	.176	.018	-.131	-.280	-.391	-.529	-.699	-.837	-1.163	-1.206	-.466	-.436
5	-.056	-.195	-.277	-.344	-.376	-.432	-.502	-.395	-.408	-.453	-.478	-.441
6	-.248	-.296	-.330	-.347	-.337	-.342	-.313	-.297	-.268	-.216	-.474	-.446
7	-.263	-.275	-.263	-.261	-.203	-.152	-.126	-.087	-.049	-.025	-.291	-.298
8	-.249	-.282	-.317	-.366	-.510	-.696	-.244	.194	.369	.560	.689	.818
9	-.257	-.298	-.324	-.371	-.490	-.561	-.068	.171	.320	.473	.572	.686
10	-.275	-.313	-.348	-.385	-.455	-.244	.049	.147	.249	.357	.434	.537
11	-.289	-.328	-.355	-.370	-.270	.015	.051	.103	.159	.224	.262	.333
12	-.263	-.306	-.320	-.286	-.053	.065	.065	.094	.124	.162	.175	.230
13	-.210	-.232	-.201	-.090	.091	.104	.096	.099	.102	.096	.037	.068

$V/c=0.80$

1	1.155	1.116	1.041	0.934	0.824	0.697	0.532	0.323	0.076	-0.205	-0.474	-0.651
2	.911	.784	.645	.495	.323	.156	-.041	-.257	-.509	-.742	-.733	-.487
3	.524	.360	.177	-.012	-.205	-.390	-.599	-.792	-.968	-.873	-.516	-.423
4	.222	.076	-.090	-.268	-.451	-.618	-.789	-.912	-.942	-.596	-.412	-.346
5	-.082	-.201	-.315	-.400	-.467	-.523	-.582	-.636	-.546	-.503	-.460	-.387
6	-.261	-.330	-.379	-.393	-.383	-.327	-.294	-.243	-.295	-.364	-.404	-.392
7	-.335	-.349	-.359	-.329	-.235	-.139	-.076	-.039	-.073	-.205	-.264	-.267
8	-.220	-.247	-.282	-.342	-.451	-.729	-.479	.136	.341	.536	.701	.838
9	-.229	-.252	-.290	-.348	-.461	-.599	-.248	.160	.310	.464	.602	.738
10	-.235	-.269	-.310	-.363	-.440	-.352	.021	.138	.243	.356	.468	.574
11	-.250	-.277	-.324	-.352	-.310	-.018	.063	.094	.147	.208	.287	.376
12	-.247	-.273	-.291	-.270	-.102	.062	.071	.087	.110	.140	.190	.252
13	-.202	-.215	-.198	-.107	.060	.117	.096	.076	.055	.041	.059	.084

$V/c=0.95$

1	1.224	1.179	1.116	1.015	0.941	0.831	0.702	0.558	0.378	0.152	-0.116	-0.436
2	.993	.879	.750	.601	.470	.330	.188	.032	-.167	-.418	-.538	-.594
3	.612	.454	.291	.128	-.027	-.169	-.314	-.438	-.574	-.627	-.571	-.535
4	.279	.118	-.063	-.221	-.363	-.465	-.554	-.664	-.536	-.468	-.348	-.276
5	-.068	-.205	-.338	-.413	-.524	-.631	-.570	-.487	-.372	-.375	-.362	-.297
6	-.277	-.366	-.441	-.518	-.607	-.581	-.423	-.376	-.387	-.429	-.388	-.305
7	-.403	-.356	-.378	-.392	-.192	-.161	-.202	-.251	-.314	-.287	-.276	-.216
8	-.224	-.244	-.254	-.258	-.575	-.895	-.651	-.058	.345	.541	.726	.879
9	-.238	-.245	-.272	-.305	-.417	-.759	-.504	.138	.314	.477	.632	.766
10	-.250	-.266	-.295	-.333	-.398	-.530	-.123	.107	.231	.370	.491	.612
11	-.263	-.279	-.310	-.353	-.319	-.044	.036	.052	.126	.214	.304	.404
12	-.253	-.259	-.279	-.280	-.215	-.075	.016	.037	.080	.132	.203	.279
13	-.219	-.219	-.219	-.173	-.070	.026	-.024	-.026	-.012	.010	.041	.090

$V/c=1.08$

1	1.268	1.227	1.169	1.089	0.991	0.901	0.810	0.678	0.523	0.333	0.102	-0.175
2	1.028	.925	.819	.709	.583	.454	.323	.193	.029	-.197	-.362	-.483
3	.676	.539	.395	.258	.133	-.001	-.131	-.242	-.388	-.464	-.506	-.508
4	.372	.233	.086	-.056	-.182	-.311	-.431	-.538	-.554	-.449	-.290	-.276
5	-.003	-.115	-.233	-.355	-.464	-.487	-.440	-.346	-.317	-.313	-.318	-.288
6	-.233	-.334	-.433	-.454	-.379	-.331	-.302	-.313	-.322	-.322	-.325	-.290
7	-.325	-.363	-.371	-.257	-.269	-.242	-.278	-.282	-.297	-.326	-.286	-.219
8	-.233	-.257	-.268	-.373	-.784	-.630	-.441	-.170	.403	.588	.764	.909
9	-.238	-.260	-.276	-.439	-.708	-.539	-.354	.058	.363	.582	.778	.814
10	-.246	-.274	-.297	-.413	-.575	-.393	-.335	.101	.264	.408	.532	.650
11	-.260	-.276	-.289	-.350	-.570	-.416	-.241	-.034	.102	.212	.311	.417
12	-.242	-.257	-.262	-.286	-.113	-.030	.041	.052	.012	.091	.164	.287
13	-.199	-.220	-.230	-.184	.004	.125	.115	.017	-.001	.001	.033	.082

OBSERVED VALUES OF  $\frac{p-p_0}{q}$ , AIRFOIL 2

$V/c=0.50$

Station	Angle of attack											
	-20°	-16°	-12°	-8°	-4°	0°	4°	8°	12°	16°	20°	24°
1	1.069	1.056	1.014	0.947	0.857	0.748	0.558	0.275	-0.106	-0.528	-1.025	-0.588
2	.858	.736	.589	.402	.245	.002	-.284	-.539	-1.025	-1.487	-1.910	-.709
3	.426	.254	.054	-.151	-.344	-.554	-.806	-1.099	-1.412	-1.704	-1.884	-.356
4	.089	-.049	-.208	-.355	-.499	-.629	-.755	-.881	-1.056	-1.380	-1.305	-.360
5	-.140	-.233	-.308	-.390	-.438	-.483	-.534	-.573	-.610	-.647	-.684	-.407
6	-.311	-.359	-.394	-.416	-.431	-.434	-.429	-.395	-.373	-.325	-.249	-.473
7	-.328	-.320	-.320	-.306	-.310	-.234	-.179	-.140	-.099	-.034	.012	-.352
8	-.276	-.285	-.310	-.344	-.444	-.679	-.453	.189	.341	.553	.717	.776
9	-.281	-.297	-.322	-.357	-.462	-.620	.066	.140	.284	.447	.586	.647
10	-.310	-.334	-.359	-.378	-.447	-.330	.033	.124	.224	.339	.449	.498
11	-.326	-.342	-.364	-.374	-.318	.017	.037	.086	.143	.209	.283	.318
12	-.308	-.324	-.327	-.294	-.127	.051	.049	.075	.114	.155	.200	.209
13	-.246	-.249	-.219	-.118	.071	.109	.099	.100	.114	.122	.132	.064

$V/c=0.65$

1	1.117	1.108	1.057	0.989	0.912	0.807	0.662	0.453	0.195	-0.121	-0.279	-0.509
2	.899	.777	.634	.460	.303	.125	-.113	-.393	-.666	-.981	-.712	-.663
3	.467	.285	.095	-.105	-.291	-.485	-.755	-1.078	-1.388	-1.447	-.396	-.385
4	.122	-.041	-.200	-.365	-.482	-.617	-.732	-.948	-1.214	-1.275	-.394	-.362
5	-.135	-.246	-.333	-.403	-.432	-.458	-.569	-.423	-.430	-.472	-.416	-.453
6	-.345	-.414	-.446	-.461	-.437	-.417	-.389	-.353	-.304	-.248	-.485	-.472
7	-.342	-.379	-.374	-.370	-.261	-.153	-.147	-.099	-.049	-.020	-.360	-.318
8	-.251	-.263	-.290	-.320	-.428	-.623	-.546	.078	.343	.529	.671	.807
9	-.251	-.275	-.312	-.355	-.438	-.579	-.120	.128	.278	.437	.539	.671
10	-.278	-.301	-.324	-.352	-.423	-.396	.012	.130	.255	.344	.419	.534
11	-.282	-.318	-.342	-.365	-.319	.002	.055	.102	.155	.219	.261	.342
12	-.267	-.297	-.308	-.294	-.127	.069	.066	.085	.120	.157	.175	.281
13	-.226	-.238	-.213	-.131	.064	.127	.112	.107	.109	.102	.044	.076

$V/c=0.80$

1	1.162	1.148	1.107	1.055	0.981	0.910	0.796	0.651	0.468	0.254	0.022	-0.246
2	.960	.852	.717	.574	.421	.274	.103	-.076	-.294	-.479	-.566	-.579
3	.526	.360	.164	-.018	-.209	-.392	-.612	-.840	-.988	-.729	-.397	-.401
4	.171	.002	-.181	-.337	-.516	-.694	-.835	-.950	-.884	-.583	-.376	-.315
5	-.129	-.246	-.355	-.444	-.510	-.617	-.742	-.788	-.546	-.493	-.405	-.352
6	-.394	-.468	-.517	-.530	-.517	-.444	-.386	-.297	-.323	-.383	-.439	-.407
7	-.441	-.470	-.462	-.390	-.285	-.159	-.078	-.050	-.119	-.295	-.303	-.288
8	-.200	-.226	-.257	-.308	-.424	-.654	-.643	-.037	.338	.522	.701	.838
9	-.206	-.230	-.270	-.321	-.435	-.606	-.287	.136	.271	.429	.583	.715
10	-.229	-.255	-.294	-.335	-.408	-.420	-.069	.124	.222	.341	.454	.568
11	-.234	-.269	-.310	-.338	-.336	-.048	.063	.087	.159	.207	.286	.370
12	-.227	-.256	-.276	-.268	-.163	.053	.069	.071	.094	.132	.184	.248
13	-.191	-.214	-.195	-.135	.030	.128	.102	.067	.042	.041	.053	.088

$V/c=0.95$

1	1.236	1.233	1.194	1.133	1.074	1.003	0.925	0.818	0.676	0.489	0.272	0.035
2	1.030	.938	.824	.686	.552	.434	.314	.179	.011	-.194	-.416	-.445
3	.610	.456	.290	.127	-.041	-.183	-.357	-.511	-.675	-.671	-.284	-.256
4	.254	.106	-.040	-.203	-.359	-.493	-.641	-.683	-.632	-.495	-.399	-.335
5	-.066	-.204	-.367	-.516	-.620	-.591	-.534	-.432	-.339	-.389	-.342	-.287
6	-.382	-.445	-.518	-.576	-.547	-.489	-.363	-.377	-.384	-.396	-.352	-.309
7	-.412	-.449	-.458	-.371	-.241	-.192	-.244	-.304	-.345	-.350	-.330	-.264
8	-.223	-.244	-.257	-.274	-.414	-.650	-.864	-.496	.239	.531	.711	.877
9	-.223	-.243	-.260	-.296	-.445	-.783	-.566	.082	.274	.440	.601	.746
10	-.240	-.266	-.282	-.304	-.389	-.618	-.316	.118	.220	.351	.475	.610
11	-.258	-.281	-.305	-.327	-.215	.015	.068	.056	.121	.208	.300	.393
12	-.240	-.270	-.272	-.279	-.259	.077	.020	.027	.065	.119	.183	.258
13	-.205	-.221	-.223	-.204	-.119	.019	-.010	-.011	.001	.026	.056	.103

$V/c=1.08$

1	1.286	1.271	1.245	1.205	1.148	1.075	0.995	0.906	0.792	0.637	0.456	0.240
2	1.102	.906	.784	.678	.559	.452	.336	.204	.021	-.183	-.339	-.339
3	.698	.564	.427	.278	.138	.003	-.163	-.286	-.389	-.524	-.602	-.229
4	.362	.233	.095	-.053	-.180	-.307	-.436	-.434	-.352	-.433	-.358	-.248
5	-.007	-.144	-.272	-.384	-.423	-.429	-.444	-.360	-.351	-.330	-.368	-.274
6	-.326	-.419	-.427	-.355	-.299	-.298	-.297	-.314	-.331	-.328	-.306	-.281
7	-.328	-.346	-.317	-.237	-.228	-.250	-.281	-.305	-.330	-.325	-.282	-.260
8	-.230	-.257	-.277	-.387	-.566	-.756	-.602	-.379	.329	.568	.741	.894
9	-.234	-.258	-.282	-.400	-.721	-.563	-.366	-.079	.311	.477	.632	.774
10	-.264	-.285	-.303	-.403	-.626	-.453	-.254	.027	.232	.379	.507	.628
11	-.261	-.277	-.298	-.378	-.583	-.432	-.254	-.068	.090	.205	.303	.411
12	-.245	-.260	-.268	-.295	-.154	-.102	-.140	.009	-.007	.070	.155	.248
13	-.200	-.217	-.221	-.208	-.087	.079	.152	.062	-.011	-.003	.033	.085

OBSERVED VALUES OF  $\frac{p-p_0}{q}$ , AIRFOIL 3

$V/c=0.50$

Station	Angle of attack											
	-20°	-16°	-12°	-8°	-4°	0°	4°	8°	12°	16°	20°	24°
1	1.057	1.054	1.022	0.963	0.891	0.801	0.645	0.411	0.103	-0.292	-0.707	-0.461
2	.895	.794	.664	.514	.353	.179	-.059	-.363	-.721	-1.107	-1.502	-0.673
3	.405	.227	.033	-.168	-.369	-.611	-.891	-1.195	-1.510	-1.756	-1.873	-.325
4	.067	-.097	-.250	-.408	-.554	-.693	-.838	-.990	-1.172	-1.420	-1.630	-.272
5	-.226	-.320	-.408	-.468	-.527	-.579	-.640	-.715	-.866	-.971	-1.032	-.385
6	-.428	-.481	-.514	-.525	-.510	-.516	-.489	-.469	-.440	-.379	-.272	-.464
7	-.321	-.347	-.385	-.394	-.308	-.163	-.142	-.102	-.050	-.003	.028	-.322
8	-.250	-.258	-.274	-.302	-.306	-.300	-.262	-.250	-.250	-.470	.644	.712
9	-.276	-.289	-.303	-.334	-.441	-.651	-.123	.138	.263	.424	.571	.636
10	-.291	-.307	-.323	-.347	-.431	-.378	.016	.104	.204	.316	.423	.482
11	-.319	-.334	-.344	-.365	-.344	-.001	.038	.088	.140	.207	.279	.317
12	-.310	-.319	-.321	-.297	-.155	.059	.056	.081	.114	.154	.199	.204
13	-.240	-.245	-.213	-.127	.052	.117	.166	.106	.113	.123	.127	.050

$V/c=0.65$

1	1.102	1.095	1.064	1.009	0.947	0.864	0.744	0.567	0.330	0.064	-0.094	-0.353
2	.935	.839	.717	.574	.434	.283	.085	-.140	-.414	-.665	-.641	-.654
3	.449	.275	.076	-.124	-.324	-.525	-.802	-1.062	-1.356	-.978	-.441	-.410
4	.094	-.071	-.240	-.396	-.537	-.681	-.867	-1.071	-1.277	-.936	-.502	-.394
5	-.226	-.341	-.434	-.502	-.550	-.614	-.691	-.598	-.510	-.504	-.457	-.427
6	-.470	-.539	-.569	-.561	-.528	-.474	-.461	-.422	-.349	-.377	-.482	-.467
7	-.393	-.426	-.447	-.369	-.217	-.134	-.095	-.041	-.004	-.275	-.341	-.330
8	-.227	-.249	-.256	-.287	-.386	-.550	-.599	-.003	.247	.455	.596	.756
9	-.247	-.270	-.286	-.322	-.432	-.581	-.317	.120	.287	.432	.542	.669
10	-.261	-.290	-.299	-.335	-.422	-.423	-.014	.126	.222	.325	.411	.521
11	-.280	-.308	-.329	-.357	-.333	-.032	.063	.097	.164	.219	.260	.337
12	-.259	-.289	-.301	-.286	-.138	.081	.080	.101	.134	.163	.180	.235
13	-.217	-.227	-.208	-.137	.054	.137	.120	.113	.113	.111	.058	.077

$V/c=0.80$

1	1.160	1.150	1.127	1.087	1.031	0.955	0.859	0.735	0.568	0.366	0.133	-0.123
2	1.012	.923	.814	.687	.562	.431	.286	.123	-.071	-.273	-.601	-.602
3	.540	.372	.186	-.007	-.193	-.369	-.562	-.756	-.772	-.601	-.398	-.335
4	.174	.011	-.165	-.347	-.542	-.768	-.956	-.974	-.773	-.514	-.349	-.311
5	-.214	-.315	-.431	-.560	-.686	-.836	-.880	-.683	-.497	-.445	-.405	-.373
6	-.503	-.508	-.546	-.591	-.554	-.501	-.390	-.370	-.439	-.434	-.434	-.404
7	-.494	-.537	-.505	-.365	-.215	-.069	-.041	-.117	-.240	-.298	-.330	-.305
8	-.188	-.209	-.240	-.276	-.372	-.583	-.672	-.110	.215	.418	.613	.776
9	-.200	-.209	-.246	-.287	-.401	-.594	-.435	.044	.256	.421	.574	.715
10	-.214	-.241	-.273	-.314	-.393	-.435	-.106	.102	.206	.317	.432	.549
11	-.233	-.269	-.288	-.333	-.336	-.119	.051	.075	.135	.200	.278	.389
12	-.232	-.254	-.263	-.250	-.152	.036	.069	.066	.091	.126	.183	.248
13	-.193	-.207	-.201	-.147	.006	.122	.084	.092	.002	.016	.042	.078

$V/c=0.95$

1	1.236	1.232	1.204	1.162	1.112	1.052	0.986	0.881	0.758	0.566	0.377	0.153
2	1.091	1.009	.918	.802	.699	.581	.439	.340	.192	-.002	-.241	-.412
3	.638	.450	.322	.161	.006	-.134	-.287	-.432	-.522	-.502	-.296	-.258
4	.276	.127	-.015	-.225	-.412	-.534	-.625	-.591	-.398	-.332	-.301	-.279
5	-.199	-.367	-.498	-.581	-.642	-.552	-.478	-.366	-.345	-.347	-.332	-.285
6	-.436	-.546	-.556	-.540	-.485	-.335	-.365	-.366	-.391	-.365	-.351	-.307
7	-.462	-.475	-.402	-.330	-.241	-.250	-.297	-.334	-.355	-.332	-.306	-.258
8	-.208	-.225	-.240	-.281	-.401	-.549	-.818	-.571	.199	.432	.644	.813
9	-.228	-.249	-.265	-.304	-.443	-.650	-.654	-.070	.273	.433	.600	.756
10	-.240	-.258	-.276	-.317	-.407	-.629	-.317	.097	.197	.333	.467	.594
11	-.259	-.280	-.297	-.324	-.368	-.017	.086	.063	.124	.207	.300	.399
12	-.251	-.271	-.292	-.301	-.282	.100	.061	.049	.081	.121	.185	.261
13	-.215	-.226	-.226	-.219	-.146	.009	-.010	.006	.010	.035	.066	.108

$V/c=1.03$

1	1.282	1.276	1.256	1.224	1.179	1.112	1.039	0.954	0.853	0.710	0.535	0.338
2	1.146	1.072	.983	.886	.785	.682	.570	.454	.332	.174	-.040	-.274
3	.722	.584	.441	.297	.164	.026	-.113	-.229	-.342	-.407	-.405	-.223
4	.377	.258	.106	-.069	-.207	-.330	-.434	-.432	-.327	-.287	-.258	-.236
5	-.099	-.229	-.347	-.442	-.513	-.367	-.366	-.338	-.305	-.299	-.275	-.254
6	-.363	-.425	-.399	-.373	-.285	-.290	-.313	-.326	-.325	-.309	-.301	-.293
7	-.338	-.326	-.305	-.269	-.229	-.261	-.302	-.319	-.323	-.323	-.275	-.236
8	-.221	-.248	-.265	-.328	-.790	-.687	-.570	-.381	.098	.477	.681	.848
9	-.236	-.260	-.281	-.343	-.774	-.625	-.440	-.181	.330	.481	.640	.786
10	-.249	-.275	-.299	-.359	-.644	-.469	-.273	.011	.209	.360	.493	.618
11	-.266	-.282	-.297	-.340	-.612	-.464	-.294	-.111	.073	.193	.309	.408
12	-.256	-.272	-.289	-.338	-.176	-.121	-.081	.042	-.007	.064	.151	.249
13	-.203	-.230	-.245	-.238	-.088	.065	.158	.089	.083	.028	.062	.107

OBSERVED VALUES OF  $\frac{p-p_0}{q}$ , AIRFOIL 4

$V/c=0.50$

Station	Angle of attack											
	-20°	-16°	-12°	-8°	-4°	0°	4°	8°	12°	16°	20°	24°
1.....	1.055	1.047	1.017	0.970	0.901	0.825	0.696	0.502	0.253	-0.048	-0.001	-0.209
2.....	.857	.733	.582	.521	.224	.015	-.247	-.571	-.952	-1.359	-.776	-.739
3.....	.397	.209	.002	-.208	-.429	-.650	-.901	-1.203	-1.511	-1.819	-.414	-.312
4.....	-.035	-.208	-.380	-.546	-.695	-.846	-.993	-1.135	-1.322	-1.513	-.381	-.324
5.....	-.287	-.385	-.482	-.548	-.602	-.649	-.713	-.744	-.762	-.754	-.413	-.369
6.....	-.675	-.717	-.736	-.721	-.668	-.638	-.660	-.675	-.588	-.468	-.487	-.453
7.....	-.410	-.444	-.474	-.478	-.328	-.152	-.123	-.062	-.014	.020	-.352	-.329
8.....	-.255	-.266	-.270	-.300	-.382	-.534	-.708	-.266	.219	.468	.572	.734
9.....	-.269	-.280	-.291	-.316	-.397	-.613	-.264	.104	.244	.408	.509	.612
10.....	-.283	-.295	-.305	-.334	-.404	-.481	.011	.091	.191	.301	.364	.471
11.....	-.312	-.329	-.332	-.350	-.362	-.085	.042	.079	.136	.198	.236	.306
12.....	-.301	-.314	-.315	-.303	-.208	.072	.060	.080	.106	.148	.138	.197
13.....	-.234	-.237	-.208	-.133	.047	.139	.107	.099	.101	.105	.003	.037

$V/c=0.65$

1.....	1.096	1.082	1.061	1.019	0.962	0.891	0.792	0.651	0.449	0.313	0.109	-0.095
2.....	.895	.770	.624	.475	.307	.112	-.120	-.365	-.662	-.718	-.793	-.737
3.....	.431	.257	.062	-.130	-.334	-.517	-.737	-1.005	-1.296	-1.184	-.436	-.392
4.....	-.015	-.200	-.381	-.544	-.701	-.851	-1.090	-1.315	-1.346	-.419	-.363	-.361
5.....	-.301	-.407	-.502	-.560	-.603	-.653	-.555	-.494	-.544	-.402	-.407	-.416
6.....	-.752	-.812	-.823	-.769	-.706	-.661	-.662	-.555	-.371	-.474	-.478	-.463
7.....	-.486	-.524	-.548	-.444	-.243	-.113	-.045	-.006	-.023	-.361	-.357	-.345
8.....	-.227	-.243	-.255	-.250	-.362	-.519	-.639	-.319	.194	.400	.611	.777
9.....	-.235	-.252	-.261	-.305	-.377	-.539	-.458	.015	.253	.401	.534	.675
10.....	-.253	-.274	-.286	-.315	-.386	-.460	-.100	.102	.204	.278	.390	.510
11.....	-.273	-.299	-.310	-.332	-.351	-.162	.059	.095	.151	.192	.255	.332
12.....	-.261	-.288	-.294	-.286	-.198	.067	.079	.089	.117	.130	.167	.221
13.....	-.212	-.224	-.208	-.139	.037	.149	.116	.096	.081	.069	.032	.055

$V/c=0.80$

1.....	1.160	1.153	1.133	1.099	1.055	0.986	0.912	0.808	0.674	0.509	0.318	0.109
2.....	.964	.851	.721	.577	.425	.280	.118	-.060	-.253	-.432	-.607	-.683
3.....	.534	.371	.194	.012	-.164	-.321	-.491	-.666	-.713	-.617	-.567	-.826
4.....	.091	-.068	-.250	-.466	-.688	-.908	-1.012	-.852	-.477	-.397	-.339	-.312
5.....	-.248	-.377	-.506	-.662	-.768	-.881	-.742	-.551	-.434	-.411	-.373	-.389
6.....	-.821	-.899	-.910	-.849	-.800	-.622	-.419	-.412	-.448	-.449	-.428	-.398
7.....	-.501	-.537	-.488	-.404	-.202	-.064	-.091	-.226	-.316	-.344	-.330	-.312
8.....	-.201	-.216	-.236	-.271	-.370	-.617	-.774	-.582	-.034	.384	.618	.792
9.....	-.204	-.219	-.247	-.276	-.362	-.563	-.592	-.178	.221	.387	.543	.691
10.....	-.179	-.214	-.247	-.280	-.335	-.463	-.230	.073	.176	.289	.408	.534
11.....	-.194	-.234	-.264	-.291	-.326	-.154	.022	.068	.137	.193	.266	.350
12.....	-.232	-.252	-.277	-.276	-.232	.002	.060	.062	.080	.122	.174	.243
13.....	-.186	-.206	-.205	-.151	-.014	.109	.050	.013	-.019	-.001	.029	.069

$V/c=0.95$

1.....	1.233	1.231	1.218	1.177	1.138	1.078	1.009	0.926	0.823	0.681	0.520	0.330
2.....	1.046	.947	.837	.711	.577	.444	.311	.169	.016	-.170	-.366	-.535
3.....	.640	.494	.345	.195	.052	-.081	-.235	-.381	-.508	-.578	-.340	-.275
4.....	.187	.017	-.173	-.367	-.529	-.643	-.627	-.435	-.343	-.309	-.262	-.260
5.....	-.178	-.347	-.493	-.580	-.620	-.535	-.406	-.353	-.338	-.323	-.289	-.261
6.....	-.664	-.693	-.632	-.526	-.396	-.326	-.341	-.371	-.387	-.361	-.348	-.302
7.....	-.532	-.480	-.428	-.353	-.266	-.290	-.314	-.346	-.360	-.320	-.306	-.265
8.....	-.224	-.245	-.263	-.299	-.416	-1.077	-.948	-.764	-.194	.376	.630	.829
9.....	-.219	-.249	-.266	-.301	-.409	-.347	-.733	-.355	.204	.394	.571	.734
10.....	-.238	-.263	-.285	-.327	-.428	-.688	-.432	.093	.175	.309	.447	.577
11.....	-.254	-.279	-.301	-.326	-.337	-.066	.080	.062	.112	.193	.284	.392
12.....	-.249	-.270	-.287	-.309	-.324	.057	.080	.055	.082	.129	.183	.267
13.....	-.205	-.226	-.239	-.234	-.177	-.021	-.022	-.024	-.006	.016	.034	.038

$V/c=1.08$

1.....	1.290	1.284	1.266	1.236	1.196	1.140	1.072	0.998	0.912	0.794	0.664	0.486
2.....	1.115	1.020	.912	.791	.673	.571	.432	.302	.175	.015	-.163	-.318
3.....	.726	.603	.469	.343	.253	.091	-.053	-.182	-.295	-.462	-.360	-.199
4.....	.289	.133	-.037	-.188	-.327	-.429	-.454	-.359	-.291	-.273	-.205	-.224
5.....	-.111	-.241	-.354	-.417	-.372	-.383	-.350	-.322	-.307	-.297	-.269	-.258
6.....	-.518	-.444	-.348	-.336	-.261	-.274	-.301	-.314	-.311	-.258	-.280	-.260
7.....	-.310	-.318	-.301	-.284	-.238	-.265	-.298	-.313	-.321	-.361	-.291	-.261
8.....	-.230	-.253	-.277	-.327	-.371	-.415	-.432	-.386	-.320	-.220	-.390	-.673
9.....	-.244	-.264	-.285	-.335	-.386	-.430	-.466	-.470	.268	.440	.604	.758
10.....	-.250	-.269	-.297	-.358	-.404	-.454	-.484	-.465	.182	.334	.472	.598
11.....	-.266	-.285	-.303	-.333	-.359	-.312	-.343	-.156	.064	.174	.286	.388
12.....	-.261	-.277	-.294	-.323	-.187	-.616	-.037	-.106	.068	.069	.140	.241
13.....	-.213	-.236	-.249	-.256	-.060	.050	.146	.082	.021	.009	.034	.081

OBSERVED VALUES OF  $\frac{p-p_o}{q}$ , AIRFOIL 5

$V/c=0.50$

Station	Angle of attack											
	-20°	-16°	-12°	-8°	-4°	0°	4°	8°	12°	16°	20°	24°
1	1.051	1.049	1.032	0.989	0.936	0.864	0.746	0.566	0.336	0.045	-0.275	-0.141
2	.904	.809	.683	.539	.380	.208	.018	-.237	-.551	-.863	-.457	-.496
3	.400	.212	.004	-.214	-.435	-.658	-.919	-1.225	-1.565	-1.912	-.458	-.313
4	-.067	-.258	-.444	-.628	-.797	-.965	-1.132	-1.278	-1.397	-1.534	-.718	-.309
5	-.393	-.497	-.688	-.863	-.970	-.974	-.817	-.592	-.461	-.345	-.658	-.344
6	-.587	-.640	-.671	-.662	-.642	-.641	-.622	-.523	-.468	-.345	-.468	-.436
7	-.473	-.517	-.541	-.530	-.471	-.436	-.383	-.321	-.260	-.201	-.154	-.323
8	-.252	-.260	-.266	-.278	-.341	-.380	-.408	-.379	-.340	-.313	-.286	-.268
9	-.250	-.269	-.273	-.292	-.376	-.405	-.432	-.419	-.340	-.286	-.253	-.258
10	-.273	-.282	-.285	-.315	-.386	-.491	-.440	-.371	-.313	-.279	-.257	-.248
11	-.301	-.309	-.317	-.336	-.357	-.479	-.441	-.370	-.315	-.289	-.259	-.291
12	-.295	-.308	-.310	-.306	-.298	-.356	-.355	-.362	-.362	-.361	-.368	-.370
13	-.224	-.223	-.203	-.139	-.000	-.151	-.119	-.105	-.103	-.103	-.099	-.021

$V/c=0.65$

1	1.098	1.094	1.076	1.040	1.002	0.938	0.844	0.711	0.538	0.349	0.133	-0.113
2	.954	.866	.756	.632	.501	.365	.196	-.012	-.214	-.359	-.404	-.610
3	.452	.279	.087	-.105	-.304	-.492	-.747	-1.047	-1.320	-1.592	-.683	-.564
4	-.041	-.227	-.426	-.608	-.789	-.910	-1.127	-1.321	-1.345	-.407	-.350	-.318
5	-.416	-.524	-.628	-.686	-.737	-.784	-.861	-.936	-.980	-.377	-.371	-.368
6	-.653	-.712	-.734	-.722	-.705	-.601	-.507	-.432	-.307	-.466	-.445	-.435
7	-.561	-.604	-.612	-.446	-.247	-.085	-.110	-.022	-.018	-.347	-.329	-.330
8	-.226	-.243	-.240	-.263	-.342	-.518	-.666	-.426	-.136	-.325	-.547	-.727
9	-.231	-.246	-.248	-.278	-.350	-.534	-.495	-.059	-.260	-.384	-.519	-.665
10	-.248	-.263	-.269	-.292	-.370	-.462	-.476	-.076	-.182	-.255	-.372	-.495
11	-.276	-.294	-.301	-.320	-.352	-.415	-.446	-.086	-.193	-.282	-.340	-.321
12	-.288	-.293	-.300	-.297	-.234	-.022	-.075	-.074	-.093	-.066	-.128	-.185
13	-.215	-.220	-.208	-.156	-.006	-.151	-.125	-.102	-.074	-.035	-.004	-.038

$V/c=0.80$

1	1.166	1.157	1.139	1.113	1.071	1.020	0.956	0.856	0.729	0.573	0.385	0.176
2	1.036	.945	.855	.743	.625	.516	.401	.268	.117	-.041	-.201	-.352
3	.564	.395	.229	.049	-.129	-.305	-.476	-.647	-.690	-.624	-.387	-.403
4	.068	-.115	-.298	-.508	-.697	-.841	-.912	-.859	-.557	-.601	-.456	-.340
5	-.323	-.448	-.643	-.803	-.901	-.897	-.786	-.683	-.516	-.428	-.399	-.376
6	-.594	-.702	-.738	-.752	-.648	-.480	-.390	-.406	-.424	-.419	-.408	-.366
7	-.564	-.606	-.571	-.468	-.212	-.121	-.200	-.280	-.344	-.358	-.324	-.298
8	-.168	-.191	-.212	-.249	-.347	-.571	-.672	-.816	-.654	-.411	-.326	-.274
9	-.202	-.214	-.235	-.268	-.376	-.577	-.625	-.625	-.487	-.249	-.390	-.551
10	-.222	-.234	-.251	-.281	-.373	-.496	-.310	-.027	-.149	-.270	-.395	-.520
11	-.235	-.250	-.288	-.310	-.353	-.289	-.000	-.059	-.108	-.183	-.260	-.352
12	-.190	-.219	-.243	-.252	-.230	-.034	.018	.028	.022	.039	.087	.149
13	-.181	-.198	-.197	-.156	-.049	.046	.015	-.019	-.036	-.020	.018	.060

$V/c=0.95$

1	1.234	1.229	1.216	1.192	1.164	1.108	1.041	0.972	0.880	0.736	0.577	0.383
2	1.112	1.046	.963	.861	.761	.659	.561	.448	.327	.184	.025	-.177
3	.683	.538	.382	.225	.071	-.080	-.228	-.360	-.477	-.518	-.459	-.391
4	.194	.032	-.129	-.304	-.435	-.534	-.566	-.518	-.436	-.610	-.620	-.368
5	-.265	-.414	-.504	-.587	-.552	-.511	-.457	-.362	-.327	-.316	-.292	-.253
6	-.535	-.542	-.524	-.475	-.346	-.212	-.340	-.358	-.364	-.368	-.331	-.287
7	-.411	-.392	-.363	-.328	-.256	-.282	-.320	-.353	-.382	-.351	-.296	-.253
8	-.229	-.245	-.277	-.332	-.431	-.584	-.960	-.799	-.342	-.373	-.592	-.798
9	-.228	-.249	-.270	-.326	-.443	-.593	-.776	-.455	-.220	-.393	-.586	-.732
10	-.241	-.264	-.289	-.332	-.439	-.651	-.455	-.067	-.154	-.286	-.423	-.558
11	-.267	-.286	-.308	-.340	-.411	-.422	-.073	.061	.102	.180	.269	.371
12	-.264	-.279	-.297	-.332	-.362	-.362	-.056	.024	.039	.086	.154	.234
13	-.214	-.231	-.246	-.249	-.223	-.056	-.020	-.025	-.012	.014	.049	.066

$V/c=1.08$

1	1.284	1.282	1.270	1.241	1.200	1.162	1.098	1.027	0.944	0.826	0.688	0.515
2	1.165	1.091	1.012	.924	.837	.747	.656	.552	.448	.327	.182	.008
3	.755	.626	.490	.356	.215	.083	-.050	-.225	-.325	-.413	-.466	-.491
4	.303	.164	.013	-.130	-.246	-.351	-.404	-.415	-.325	-.295	-.264	-.228
5	-.159	-.277	-.409	-.425	-.356	-.339	-.336	-.342	-.299	-.287	-.262	-.242
6	-.348	-.319	-.332	-.293	-.254	-.270	-.302	-.321	-.315	-.303	-.290	-.269
7	-.366	-.329	-.326	-.269	-.245	-.282	-.294	-.314	-.291	-.276	-.244	-.212
8	-.233	-.254	-.274	-.298	-.385	-.521	-.704	-.558	-.352	-.340	-.614	-.824
9	-.236	-.254	-.273	-.303	-.344	-.476	-.558	-.339	-.241	-.436	-.598	-.760
10	-.249	-.269	-.289	-.325	-.375	-.534	-.399	-.144	.156	.305	.454	.588
11	-.274	-.293	-.307	-.335	-.404	-.536	-.368	-.180	.041	.159	.270	.373
12	-.270	-.280	-.299	-.350	-.226	-.156	-.123	.017	.005	.030	.125	.220
13	-.215	-.242	-.264	-.270	-.078	-.044	-.143	.111	.028	.020	.048	.090

OBSERVED VALUES OF  $\frac{p-p_0}{q}$ , AIRFOIL 6

$V/c=0.50$

Station	Angle of attack											
	-20°	-16°	-12°	-8°	-4°	0°	4°	8°	12°	16°	20°	24°
1	1.050	1.047	1.037	1.007	0.966	0.908	0.830	0.693	0.511	0.288	0.008	0.119
2	.926	.835	.718	.588	.445	.275	.089	-.161	-.451	-.768	-1.093	-.507
3	.421	.232	.032	-.178	-.393	-.606	-.858	-1.167	-1.490	-1.824	-.634	-.265
4	-.124	-.302	-.489	-.678	-.844	-.992	-1.151	-1.301	-1.454	-1.630	-.325	-.278
5	-.473	-.576	-.667	-.738	-.788	-.830	-.889	-.988	-.727	-.736	-.611	-.332
6	-.688	-.740	-.766	-.751	-.729	-.718	-.634	-.575	-.505	-.405	-.237	-.429
7	-.552	-.600	-.628	-.571	-.276	-.143	-.072	-.028	-.019	-.007	-.076	-.298
8	-.239	-.246	-.237	-.248	-.317	-.471	-.680	-.491	-.067	-.365	.468	.657
9	-.244	-.257	-.252	-.264	-.327	-.522	-.548	.033	.227	.338	.422	.564
10	-.267	-.271	-.269	-.279	-.332	-.455	-.213	.064	.152	.259	.363	.426
11	-.292	-.296	-.296	-.316	-.349	-.232	.048	.067	.120	.179	.205	.283
12	-.281	-.285	-.285	-.293	-.231	.023	.063	.067	.096	.134	.116	.173
13	-.217	-.220	-.206	-.159	-.035	.163	.125	.106	.104	.101	.091	.022

$V/c=0.65$

1	1.106	1.102	1.095	1.071	1.035	0.986	0.919	0.820	0.691	0.582	0.415	0.230
2	.973	.902	.807	.688	.557	.419	.263	.064	-.123	-.195	-.340	-.457
3	.498	.329	.148	-.043	-.235	-.424	-.626	-.876	-1.016	-.700	-.564	-.304
4	-.090	-.271	-.458	-.650	-.824	-1.006	-1.156	-1.335	-1.323	-.463	-.386	-.341
5	-.488	-.610	-.701	-.787	-.852	-.898	-1.005	-.985	-.671	-.372	-.351	-.324
6	-.767	-.816	-.819	-.804	-.784	-.653	-.534	-.434	-.312	-.448	-.411	-.361
7	-.665	-.698	-.651	-.467	-.267	-.063	-.012	.018	-.286	-.370	-.346	-.300
8	-.216	-.228	-.223	-.245	-.311	-.442	-.622	-.549	-.039	.232	.484	.688
9	-.220	-.225	-.226	-.251	-.340	-.496	-.586	-.115	.205	.323	.463	.605
10	-.237	-.252	-.250	-.268	-.339	-.453	-.309	.069	.155	.235	.343	.464
11	-.247	-.260	-.269	-.301	-.345	-.240	.061	.086	.126	.174	.231	.314
12	-.258	-.265	-.250	-.261	-.215	.007	.086	.081	.086	.084	.134	.197
13	-.186	-.199	-.189	-.156	.022	.149	.127	.093	.064	-.007	.017	.049

$V/c=0.80$

1	1.158	1.155	1.149	1.130	1.102	1.068	1.008	0.931	0.835	0.716	0.565	0.394
2	1.066	.992	.905	.794	.683	.571	.450	.310	.161	.002	-.159	-.311
3	.612	.463	.278	.118	-.032	-.184	-.325	-.483	-.578	-.570	-.404	-.277
4	.029	-.161	-.353	-.550	-.760	-.888	-.924	-.854	-.502	-.378	-.312	-.304
5	-.433	-.593	-.756	-.883	-.924	-.866	-.660	-.545	-.426	-.379	-.353	-.302
6	-.736	-.802	-.838	-.887	-.632	-.427	-.401	-.415	-.434	-.425	-.408	-.366
7	-.557	-.572	-.548	-.425	-.223	-.192	-.256	-.324	-.354	-.349	-.337	-.297
8	-.172	-.187	-.208	-.241	-.360	-.562	-.774	-.677	-.239	.310	.543	.758
9	-.176	-.186	-.200	-.241	-.371	-.646	-.695	-.366	.163	.344	.510	.668
10	-.188	-.198	-.227	-.259	-.367	-.524	-.296	-.027	.151	.264	.387	.511
11	-.194	-.214	-.245	-.284	-.393	-.307	-.002	.062	.111	.186	.262	.347
12	-.228	-.243	-.254	-.269	-.271	-.092	.030	.032	.059	.104	.154	.221
13	-.150	-.171	-.184	-.180	-.088	.036	.000	-.025	-.021	.000	.033	.066

$V/c=0.95$

1	1.230	1.223	1.221	1.206	1.182	1.148	1.102	1.048	0.975	0.868	0.729	0.571
2	1.143	1.077	1.000	.910	.811	.705	.591	.476	.356	.219	.065	-.111
3	.724	.592	.447	.297	.158	.031	-.100	-.270	-.428	-.468	-.287	-.230
4	.168	.006	-.175	-.347	-.499	-.592	-.552	-.595	-.703	-.358	-.275	-.282
5	-.357	-.473	-.589	-.653	-.587	-.387	-.348	-.333	-.325	-.342	-.294	-.264
6	-.514	-.510	-.493	-.411	-.304	-.301	-.333	-.350	-.363	-.348	-.323	-.302
7	-.353	-.352	-.368	-.315	-.258	-.292	-.326	-.342	-.341	-.310	-.299	-.269
8	-.226	-.246	-.269	-.322	-.428	-.1093	-1.014	-.857	-.454	-.208	.535	.759
9	-.231	-.249	-.266	-.315	-.417	-.1032	-.900	-.667	.002	.361	.520	.684
10	-.248	-.265	-.289	-.343	-.433	-.532	-.574	-.010	.137	.267	.404	.534
11	-.259	-.279	-.302	-.340	-.419	-.152	.072	.077	.112	.188	.277	.364
12	-.260	-.277	-.304	-.342	-.333	-.032	.071	.035	.062	.103	.162	.235
13	-.224	-.235	-.252	-.261	-.285	-.102	-.014	-.014	.000	.027	.058	.098

$V/c=1.08$

1	1.284	1.293	1.296	1.277	1.243	1.197	1.150	1.097	1.036	0.941	0.827	0.763
2	1.197	1.139	1.068	.980	.889	.790	.685	.583	.478	.358	.223	.053
3	.791	.669	.540	.419	.291	.171	.044	-.123	-.268	-.371	-.390	-.185
4	.264	.110	-.045	-.193	-.328	-.435	-.415	-.309	-.294	-.297	-.244	-.221
5	-.246	-.372	-.469	-.480	-.404	-.304	-.279	-.283	-.265	-.246	-.229	-.216
6	-.342	-.350	-.343	-.305	-.254	-.281	-.291	-.297	-.299	-.283	-.275	-.252
7	-.321	-.315	-.307	-.287	-.248	-.269	-.294	-.309	-.297	-.283	-.261	-.249
8	-.228	-.252	-.266	-.307	-.428	-.865	-.760	-.466	-.448	.220	.562	.784
9	-.230	-.252	-.268	-.315	-.439	-.783	-.642	-.439	-.125	.396	.544	.708
10	-.254	-.275	-.290	-.334	-.474	-.621	-.449	-.219	.101	.269	.420	.548
11	-.268	-.285	-.299	-.334	-.453	-.566	-.389	-.192	.060	.164	.279	.371
12	-.260	-.279	-.291	-.320	-.241	-.140	-.107	.068	.069	.060	.198	.232
13	-.228	-.249	-.274	-.293	-.189	-.034	.127	.126	.030	.040	.061	.113

LIFT COEFFICIENTS,  $C_L$

AIRFOIL 1

$V/c$	Angle of attack											
	-20°	-16°	-12°	-8°	-4°	0°	4°	8°	12°	16°	20°	24°
0.50	-0.201	-0.177	-0.139	-0.060	0.075	0.215	0.401	0.522	0.646	0.761	0.830	0.705
.65	-.184	-.157	-.114	-.037	.070	.214	.390	.496	.629	.713	.657	.673
.80	-.150	-.106	-.058	.003	.054	.205	.354	.484	.559	.608	.626	.648
.95	-.132	-.110	-.046	.024	.027	.158	.263	.379	.458	.522	.579	.613
1.08	-.213	-.161	-.106	-.124	-.136	.040	.148	.289	.409	.491	.542	.597

AIRFOIL 2

0.50	-0.148	-0.120	-0.074	0.007	0.135	0.256	0.408	0.553	0.651	0.794	0.851	0.639
.65	-.125	-.075	-.022	.042	.095	.238	.391	.518	.622	.700	.604	.663
.80	-.054	-.011	.036	.067	.129	.243	.361	.487	.536	.573	.572	.614
.95	-.114	-.064	.000	.035	.068	.098	.186	.336	.460	.506	.545	.574
1.08	-.192	-.144	-.119	-.136	-.198	-.035	.123	.232	.353	.459	.529	.539

AIRFOIL 3

0.50	-0.098	-0.047	0.020	0.093	0.196	0.282	0.431	0.580	0.663	0.786	0.881	0.586
.65	-.045	.007	.064	.094	.144	.268	.415	.531	.619	.682	.610	.638
.80	-.007	.056	.080	.103	.152	.260	.369	.465	.498	.516	.549	.595
.95	-.063	-.001	.012	.023	.019	.087	.197	.299	.395	.453	.513	.549
1.08	-.159	-.136	-.119	-.121	-.205	-.062	.106	.221	.310	.402	.470	.518

AIRFOIL 4

0.50	0.024	0.069	0.140	0.199	0.237	0.320	0.476	0.550	0.684	0.795	0.836	0.562
.65	.079	.133	.191	.199	.209	.297	.405	.496	.617	.659	.550	.606
.80	.102	.149	.174	.217	.216	0.253, 0.265	.313	.378	.411	.480	.525	.604
.95	.021	.039	.054	.056	.089	.096	.143	.229	.335	.419	.465	.519
1.08	-.124	-.110	-.102	-.106	-.229	-.088	.060	.159	.267	.358	.431	.525

AIRFOIL 5

0.50	0.066	0.131	0.201	0.257	0.238	0.338	0.490	0.603	0.665	0.778	0.900, 0.821	0.521
.65	.123	.181	.242	.232	.233	.299	.454	.528	.591	.475	.515	.575
.80	.111	.176	.222	.256	.208	0.214, 0.178	.266	.344	.388	.476	.501	.540
.95	-.027	-.001	.008	.000	-.074	-.001	.121	.221	.307	.447	.499	.512
1.08	-.118	-.122	-.094	-.121	-.260	-.133	.010	.152	.217	.333	.410	.487

AIRFOIL 6

0.50	0.150	0.218	0.285	0.316	0.284	0.371	0.470	0.585	0.668	0.794	0.488	0.469
.65	.225	.263	.314	.296	.308	.329	.426	.532	.616	.446	.473	.490
.80	.187	.241	.280	.286	.198	0.190, 0.210	.264	.329	.358	.423	.462	.494
.95	-.010	.013	.028	.000	-.089	-.046	.060	.190	.310	.366	.405	.465
1.08	-.103	-.088	-.075	-.102	-.262	-.133, -.171	-.039	.098	.181	.304	.381	.423

DRAG COEFFICIENTS,  $C_D$ 

## AIRFOIL 1

Y/c	Angle of attack											
	-20°	-16°	-12°	-8°	-4°	0°	4°	8°	12°	16°	20°	24°
0.50	0.185	0.149	0.124	0.079	0.053	0.042	0.045	0.059	0.085	0.123	0.165	0.286
.65	.181	.151	.117	.083	.057	.044	.047	.063	.095	.140	.230	.291
.80	.180	.148	.119	.086	.068	.050	.057	.080	.119	.174	.231	.287
.95	.197	.160	.131	.105	.083	.071	.082	.107	.144	.183	.233	.275
1.08	.217	.179	.148	.124	.101	.083	.088	.108	.144	.190	.235	.284

## AIRFOIL 2

0.50	0.196	0.164	0.132	0.101	0.079	0.065	0.067	0.086	0.106	0.152	0.188	0.298
.65	.194	.163	.133	.107	.079	.067	.072	.085	.110	.156	.249	.314
.80	.186	.161	.136	.115	.092	.086	.079	.102	.138	.205	.251	.301
.95	.214	.185	.157	.133	.110	.096	.102	.127	.173	.220	.263	.303
1.08	.241	.206	.179	.157	.134	.110	.109	.128	.166	.208	.255	.302

## AIRFOIL 3

0.50	0.202	0.168	0.139	0.115	0.092	0.075	0.078	0.097	0.112	0.150	0.203	0.280
.65	.196	.170	.147	.123	.095	.081	.083	.098	.117	.210	.266	.314
.80	.197	.176	.158	.136	.110	.092	.095	.122	.166	.209	.262	.311
.95	.230	.200	.179	.157	.135	.118	.122	.139	.173	.207	.262	.302
1.08	.260	.232	.204	.179	.159	.131	.133	.145	.168	.207	.249	.303

## AIRFOIL 4

0.50	0.194	0.172	0.148	0.130	0.101	0.079	0.088	0.091	0.116	0.150	0.257	0.298
.65	.192	.172	.157	.136	.105	.089	.088	.096	.126	.202	.271	.327
.80	.199	.184	.169	.150	.123	.104	.110	.141	.178	.226	.268	.312
.95	.243	.220	.199	.183	.160	.147	.149	.163	.190	.220	.271	.319
1.08	.278	.252	.228	.205	.186	.157	.153	.163	.186	.223	.270	.338

## AIRFOIL 5

0.50	0.212	0.189	0.167	0.151	0.112	0.090	0.093	0.099	0.105	0.135	0.313, 0.175	0.289
.65	.214	.198	.183	.153	.127	.101	.112	.105	.127	.203	.247	.304
.80	.231	.213	.193	.178	.145	.128	.139	.160	.193	.240	.282	.321
.95	.276	.250	.230	.210	.188	.170	.168	.185	.205	.253	.289	.318
1.08	.309	.283	.255	.230	.209	.178	.168	.173	.194	.225	.260	.307

## AIRFOIL 6

0.50	0.224	0.205	0.194	0.176	0.135	0.122	0.109	0.111	0.125	0.169	0.193	0.302
.65	.228	.216	.207	.183	.150	.119	.118	.134	.206	.241	.273	.317
.80	.240	.225	.213	.202	.176	.162	.178	.195	.215	.254	.300	.340
.95	.298	.274	.259	.237	.215	.199	.194	.203	.227	.265	.298	.341
1.08	.330	.304	.280	.261	.238	0.208, 0.211	.196	.200	.211	.245	.285	.347

MOMENT COEFFICIENTS

AIRFOIL 1

V/c	Angle of attack											
	-20°	-16°	-12°	-8°	-4°	0°	4°	8°	12°	16°	20°	24°
0.50	-0.041	-0.030	-0.019	0.026	0.112	0.156	0.173	0.184	0.199	0.208	0.209	0.268
.65	-.028	-.019	.000	.043	.113	.155	.174	.174	.198	.196	.258	.277
.80	.000	.017	.039	.067	.097	.155	.166	.171	.183	.220	.251	.266
.95	.010	.022	.049	.082	.081	.164	.167	.178	.205	.223	.242	.242
1.08	-.022	.006	.030	.017	.052	.125	.158	.166	.181	.211	.228	.239

AIRFOIL 2

0.50	-0.013	-0.003	0.019	0.059	0.144	0.193	0.198	0.212	0.217	0.227	0.222	0.283
.65	.004	.028	.050	.081	.128	.178	.197	.188	.199	.204	.270	.295
.80	.053	.072	.092	.100	.138	.182	.186	.184	.192	.243	.254	.269
.95	.028	.052	.078	.081	.091	.148	.160	.188	.217	.239	.252	.255
1.08	-.011	.012	.017	-.005	.028	.097	.154	.172	.183	.208	.228	.243

AIRFOIL 3

0.50	0.005	0.028	0.065	0.104	0.152	0.188	0.211	0.223	0.218	0.228	0.233	0.261
.65	.045	.068	.093	.100	.130	.183	.205	.199	.199	.274	.273	.284
.80	.084	.103	.113	.168	.130	.174	.184	.193	.211	.229	.255	.269
.95	.054	.081	.075	.068	.066	.148	.173	.193	.210	.224	.244	.252
1.08	.000	.007	.009	.003	.023	.085	.157	.179	.180	.203	.220	.241

AIRFOIL 4

0.50	0.065	0.092	0.125	0.156	0.174	0.207	0.231	0.216	0.223	0.228	0.248	0.256
.65	.109	.132	.159	.153	.153	.194	.200	.190	.199	.245	.260	.279
.80	.127	.151	.152	.158	.150	0.198, .205	.175	.196	.208	.229	.246	.260
.95	.099	.095	.091	.080	.171	.137	.163	.181	.201	.209	.230	.247
1.08	.007	.012	.017	.005	.013	.077	.144	.168	.176	.188	.210	.232

AIRFOIL 5

0.50	0.090	0.121	0.154	0.179	0.156	0.208	0.233	0.228	0.209	0.219	0.260, 0.272	0.240
.65	.129	.159	.182	.160	.155	.190	.233	.205	.195	.217	.232	.257
.80	.132	.163	.176	.180	.138	0.141, .151	.174	.193	.203	.226	.240	.251
.95	.055	.062	.058	.048	.016	.114	.162	.180	.195	.223	.233	.239
1.08	.007	.002	.010	-.009	.000	.067	.129	.171	.165	.179	.199	.222

AIRFOIL 6

0.50	0.135	0.167	0.197	0.205	0.165	0.222	0.233	0.226	0.220	0.241	0.185	0.229
.65	.188	.214	.218	.190	.192	.197	.211	.213	.261	.229	.234	.238
.80	.160	.187	.190	.184	.128	.158	.185	.204	.222	.224	.242	.248
.95	.032	.063	.063	.043	-.003	.087	.151	.178	.199	.208	.232	.243
1.08	.073	.009	.012	-.003	-.011	0.042, .058	.114	.162	.167	.180	.204	.230

## CENTER OF PRESSURE COEFFICIENTS

## AIRFOIL 1

V/c	Angle of attack											
	-20°	-16°	-12°	-8°	-4°	0°	4°	8°	12°	16°	20°	24°
0.50	0.16	-0.14	0.12	-0.37	1.58	0.73	0.43	0.35	0.31	0.27	0.25	0.35
.65	.12	-.10	.00	-.90	1.71	.72	.44	.35	.31	.27	.27	.37
.80	.00	-.12	-.43	-7.44	1.98	.76	.47	.35	.32	.27	.25	.38
.95	-.05	-.15	-.67	9.11	3.86	1.04	.65	.46	.43	.40	.39	.36
1.08	.08	-.03	-.22	-.12	-.37	3.13	1.03	.55	.42	.40	.39	.36

## AIRFOIL 2

0.50	0.06	0.02	-0.20	-8.43	1.12	0.75	0.48	0.38	0.33	0.28	0.26	0.40
.65	-.02	-.24	-1.02	3.11	1.27	.75	.50	.36	.32	.28	.41	.40
.80	-.47	-1.31	13.14	1.96	1.13	.75	.51	.37	.35	.40	.41	.39
.95	-.16	-.46	-2.33	5.06	1.52	1.51	.79	.54	.45	.44	.42	.39
1.08	.04	-.06	-.11	.03	-.14	-2.77	1.18	.70	.48	.42	.39	.40

## AIRFOIL 3

0.50	-0.03	-0.30	-7.22	1.37	0.80	0.67	0.49	0.38	0.32	0.29	0.26	0.40
.65	-.41	-1.66	2.82	1.32	.95	.68	.49	.37	.32	.38	.41	.40
.80	-1.38	17.16	2.51	1.30	.90	.67	.49	.40	.40	.41	.42	.40
.95	-.39	-1.45	-2.88	68.03	6.60	1.70	.84	.61	.50	.46	.43	.40
1.08	.00	-.04	-.06	-.02	-.11	-1.37	1.37	.75	.53	.46	.42	.40

## AIRFOIL 4

0.50	-1.48	4.84	1.18	0.87	0.76	0.65	0.48	0.39	0.32	0.28	0.42	0.40
.65	13.62	1.65	1.03	.86	.76	.65	.49	.38	.32	.41	.43	.41
.80	4.54	1.62	1.13	.81	.72	.75	.55	.50	.47	.44	.42	.40
.95	-1.57	-4.13	8.27	2.67	-6.45	3.72	1.07	.72	.55	.45	.43	.41
1.08	-.03	-.07	-.12	-.04	-.05	-.88	2.06	.93	.61	.46	.42	.38

## AIRFOIL 5

0.50	-8.18	1.64	0.95	0.77	0.68	0.62	0.47	0.37	0.31	0.28	0.29, 0.31	0.41
.65	3.00	1.33	.92	.77	.69	.64	.51	.38	.32	.42	.41	.40
.80	5.28	1.48	1.00	.79	.70	0.70	.63	.53	.49	.43	.42	.40
.95	-.42	-.89	-1.45	-1.65	-1.18	-114.00	1.23	.73	.57	.45	.41	.40
1.08	-.03	-.01	-.07	.03	.03	-.50	5.83	.93	.65	.47	.42	.40

## AIRFOIL 6

0.50	2.11	1.09	0.83	0.71	0.60	0.60	0.49	0.38	0.32	0.30	0.35	0.42
.65	1.41	1.01	.83	.71	.65	.62	.49	.39	.40	.46	.43	.41
.80	1.70	1.10	.83	.72	.69	0.75	.67	.58	.56	.47	.45	.42
.95	-.46	-.93	-2.33	-1.30	.03	-1.89	2.07	.82	.57	.49	.48	.43
1.08	-.01	-.05	-.09	.02	.04	-.32	-4.56	1.30	.76	.51, .50	.45	.44